JOURNAL OF QUATERNARY SCIENCE (2023) **38**(8) 1337–1356 ISSN 0267-8179. DOI: 10.1002/jqs.3552

JQS Journal of Quaternary Science QRA Quaternary Research Association

Changing food webs before and during the Last Glacial Maximum based on stable isotopes of animal bone collagen from Lower Austria

LILIAN REISS,[1]* CHRISTOPH MAYR,[1,2] KERSTIN PASDA,[3] THOMAS EINWÖGERER,[4] MARC HÄNDEL,[4] ANDREAS LÜCKE,[5] ANDREAS MAIER[6] and HOLGER WISSEL[5]

[1]Institute of Geography, Friedrich-Alexander-Universität Erlangen-Nürnberg, Wetterkreuz 15, Erlangen, Germany
[2]Department Earth and Environmental Sciences & GeoBio-Center, Ludwig-Maximilians-Universität München, Richard-Wagner-Straße 10, Munich, Germany
[3]Institute of Prehistory and Protohistory, Friedrich-Alexander-Universität Erlangen-Nürnberg, Kochstraße 4/18, Erlangen, Germany
[4]Austrian Archaeological Institute, Austrian Academy of Sciences, Georg-Coch-Platz 2, Vienna, Austria
[5]Institute of Bio- and Geosciences, IBG-3: Agrosphäre, Forschungszentrum Jülich GmbH, Jülich, Germany
[6]Institute for Prehistoric Archaeology, University of Cologne, Bernhard-Feilchenfeld-Straße 11, Cologne, Germany

Received 3 March 2023; Revised 25 May 2023; Accepted 5 June 2023

ABSTRACT: We investigated palaeofood web structures using stable isotope analyses on animal bone collagen from four Upper Palaeolithic sites dated to the Early Gravettian (Krems-Hundssteig and Krems-Wachtberg: 33–31k cal a BP, Langenlois: 31–29k cal a BP) and to the Early Epigravettian (Kammern-Grubgraben: 24–20k cal a BP). In both periods, $\delta^{13}C$ values show niche partitioning between hare, horse and mammoth on one side, and reindeer and ibex on the other, indicating different diets and habitats between both herbivore groups. The $\delta^{15}N$ differences between carnivores and herbivores suggest a difference of one trophic level during the pre-Last Glacial Maximum (pre-LGM) period at the Early Gravettian sites and a tendency towards secondary carnivores during the LGM at Kammern-Grubgraben. $\delta^{15}N$ values of pre-LGM mammoths are elevated in relation to other herbivores but shifted to the level of other herbivores in the LGM. A general $\delta^{15}N$ value shift in herbivores of 3.3‰ from the pre-LGM to the LGM is related to climatic deterioration. This may have led to the disappearance of certain ecological niches and to a shift from broader to overlapping ecological herbivore niches shortly before the LGM, as demonstrated by SIBER analyses.

KEYWORDS: $\delta^{13}C$; $\delta^{15}N$; Epigravettian; Gravettian; niche partitioning

Introduction

Animal bones represent a frequently well-preserved and widely abundant archive at Palaeolithic sites. Their isotopic composition is commonly used to reconstruct local palaeofood webs and past ecosystems (Bocherens *et al.*, 2015; Brock *et al.*, 2010; Drucker *et al.*, 2012; DeNiro and Epstein, 1978; Hobson, 1999; Hoke *et al.*, 2019). The reconstruction of food webs is based on the fact that isotopic fractionation occurs between animals from different trophic levels. Moreover, isotopic differences at the baseline of food webs occur across geographical regions and in different climates. Potential shifts in the isotopic composition due to trophic level or geographic origin are well reflected in animal tissues, such as bone collagen (DeNiro and Epstein, 1978; Hobson, 1999).

For bone collagen, carbon stable isotopes show a trophic enrichment of approximately 0.8–1.3‰ in carnivores in comparison to their prey (Bocherens and Drucker, 2003; Krajcarz *et al.*, 2016), whereas nitrogen stable isotopes increase by about 3.0–5.0‰ per trophic level (DeNiro and Epstein, 1981; Schoeninger and DeNiro, 1984; Bocherens and Drucker, 2003; Fox-Dobbs *et al.*, 2007). Unlike tooth dentin with its incremental growth, bone is a renewing tissue, so its isotopic composition exhibits an averaged value over several years of nutritional behaviour (Drucker 2022). The collagen in the femoral bones of human adults, for instance, reflects a period of more than a decade (Hedges *et al.*, 2007).

A number of stable isotope studies on bone collagen have been conducted for the frequently prevailing steppe- and tundra-like ecosystems of the last glacial period in central Europe, in particular for Marine Isotope Stage (MIS) 3 (59–29k cal a BP) and MIS 2 (29–11.7k cal a BP) (Voelker *et al.*, 2002). Due to the predominance of large herbivorous mammals, this ecosystem is also known as 'mammoth steppe' (e.g. Zimov *et al.*, 1995, 2012; Bocherens, 2003; Bocherens *et al.*, 2005, 2014, 2015; Drucker *et al.*, 2003; Drucker and Henry-Gambier, 2005; Fox-Dobbs *et al.*, 2008; Yeakel *et al.*, 2013, Schwartz-Narbonne *et al.*, 2019). This biome is characterised by a large biomass of plants and herbivores despite the partly very cold and dry conditions during the last glacial. It has been proposed that high insolation and low humidity led to increased summer snowmelt and a longer growing season (Guthrie, 1982; Zimov *et al.*, 2012; Drucker, 2022). A rapid turnover of nutrients in loess sediments may also have favoured high vegetation productivity and, thus, provided a base for grazing and browsing by animal communities, which in turn fertilised the soils through manure and carcasses (Zimov *et al.*, 1995; Drucker, 2022). Depending on the geographic region and the time period considered, the Eurasian mammoth steppe is characterised by a changing

*Correspondence: Lilian Reiss, as above.
Email: lilian.reiss@fau.de

landscape of continuous and discontinuous permafrost (Delisle *et al.*, 2007; Blaser *et al.*, 2010; Vandenberghe *et al.*, 2014). According to Říčánková *et al.* (2015), the Altai-Sayan, Kazakhstan, and the Eastern European Plain are the areas that best serve as modern equivalents.

The isotopic composition of a number of faunal assemblages from the late MIS 3 and MIS 2 suggests a particular niche partitioning. This may have been caused by the great diversity of coexisting herbivores and interspecies competition (Iacumin *et al.*, 2000, 2006; Drucker *et al.*, 2003; Bocherens *et al.*, 2015; Drucker, 2022). Based on $\delta^{15}N$ and $\delta^{13}C$ value ranges, the ecological niches of mammoth, horse and reindeer were most frequently investigated in different regions. Most studies on faunal composition and food web structures use material from Gravettian (33–25 ka) and Magdalenian (20–14 ka) sites (Iacumin *et al.*, 2000, 2006, 2010; Drucker *et al.*, 2003, 2018; Stevens and Hedges, 2004; Stevens *et al.*, 2008; Bocherens *et al.*, 2015; Krajcarz *et al.*, 2016; Fox-Dobbs *et al.*, 2008) and thus focus on the periods before and after the Last Glacial Maximum (LGM). Here we use Mix *et al.*, (2001) definition of the LGM *sensu stricto*, which sets it at 23–19k cal a BP. Studies of the food web structure for the LGM are largely absent. From an archaeological perspective, the transition from the Gravettian to the Epigravettian is of great interest, as the human population in central Europe decreased massively and human occupation remained at very low numbers and densities in the research area during the LGM (Maier *et al.*, 2021).

The aim of this study is to infer possible food web changes related to climatic and environmental trends around the LGM using the carbon and nitrogen stable isotopes of animal bone collagen. For this purpose, we use the diverse faunal assemblages from several well-known Upper Palaeolithic sites in and near the city of Krems (Lower Austria), which date to 33–29k cal a BP (Early Gravettian/pre-LGM) and 24–20k cal a BP (Early Epigravettian/LGM). The geographic proximity of the sites allows meaningful conclusions to be drawn from a comparison between the different age periods.

Study sites

Krems-Hundssteig 2000–2002 and Krems-Wachtberg 1930 (33–31k cal a BP)

The Upper Palaeolithic sites of Krems-Hundssteig and Krems-Wachtberg are located very close to one another, both in the present-day urban area of the city of Krems (Fig. 1). Topographically, the sites are situated at the transition from the narrow Danube passage of the Wachau to the so-called Tullnerfeld, an extensive alluvial plain. They are located in the lower southern to south-eastern part (Wachtberg) of a spur-shaped promontory that rises up to 398 m a.s.l. on the northern bank of the Danube. The Wachtberg area, where loess deposits are up to 20 m thick, is slightly sloping to the southeast, thus providing wind-sheltered conditions for temporarily used campsites of hunter-gatherer communities (Händel, 2017).

The Upper Palaeolithic site of Krems-Hundssteig first received attention in the late 19th century. At that time, numerous lithic artefacts and faunal remains were found in the course of large-scale quarrying of loess sediments. The lithic industry points to the Aurignacian and Gravettian. New excavations were carried out adjacent to the former quarry area between 2000 and 2002 and identified five basic archaeological horizons (AHs). The main Upper Palaeolithic horizon, AH 3, is attributed to the Gravettian and represents a sequence of layers that can be subdivided in an upper (AH 3.1 and AH 3.2), middle (AH 3.3–AH 3.4) and lower sequence (AH 3.5–AH 3.8) (Neugebauer-Maresch *et al.*, 2008). All bone samples analysed herein originate from the Krems-Hundssteig 2000–2002 excavations and stem from AH 3.2 and 3.4, which date between 32.9 and 31.0k cal a BP (Fig. 2a). Radiocarbon dating from two lower horizons, accessed only by sounding and core sampling, exhibited age ranges of 38.9–34.5k cal a BP for AH 4 and 46.6–42.4k cal a BP for AH 5 (Neugebauer-Maresch *et al.*, 2008; Händel 2017). From a zooarchaeological point of view, Krems-Hundssteig 2000–2002 is mainly characterised by a low density of carnivores in contrast to the neighbouring Krems-Wachtberg sites (Fladerer and Salcher-Jedrasiak, 2008). The faunal

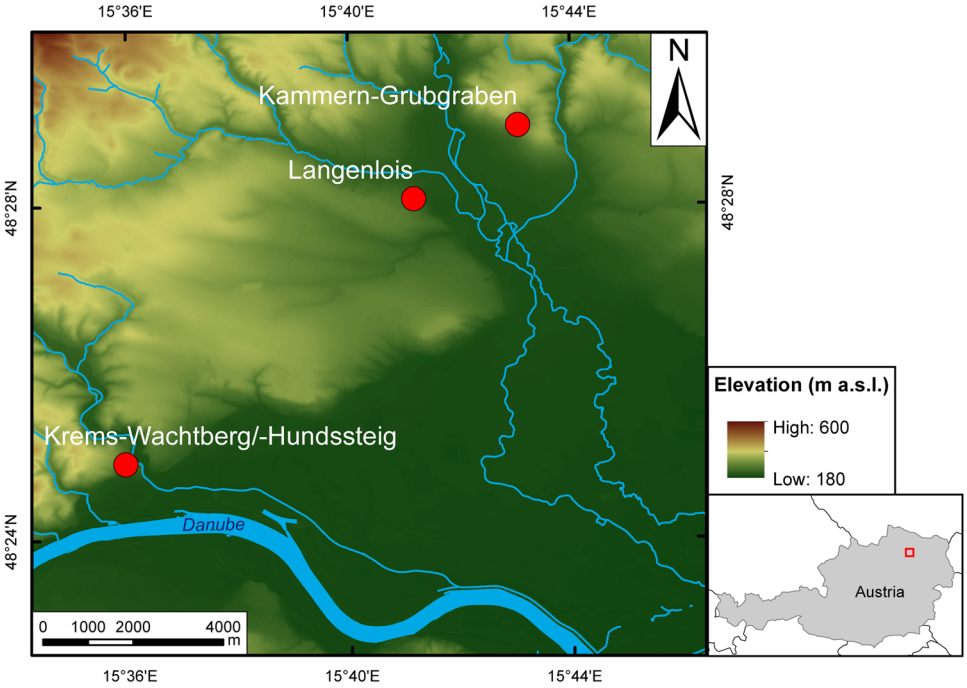

Figure 1. Location of the study sites in Lower Austria. The study sites are indicated by red dots. A digital elevation model in 10 × 10 m resolution (www.data.gv.at/katalog/dataset/land-noe-digitales-hohenmodel-10-m#resources) served as base map.

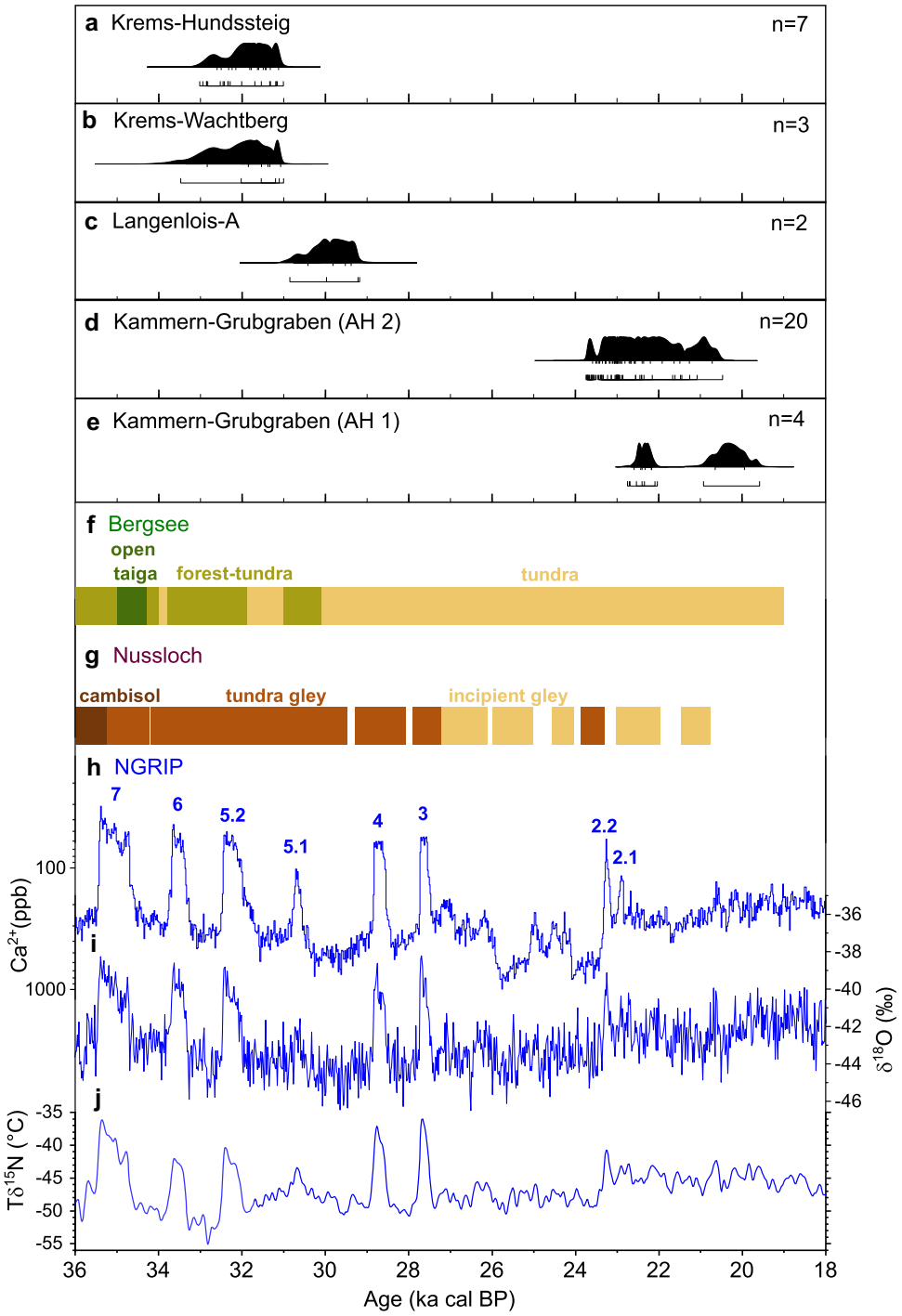

Figure 2. Published radiocarbon data from (a) Krems-Hundssteig (Neugebauer-Maresch and Stadler, 2008; Händel, 2017), (b) Krems-Wachtberg (Heinrich, 1973; Einwögerer, 2000; Händel, 2017), (c) Langenlois A (Einwögerer, 2019), and from archaeological horizon (AH) 2 (d) and AH 1 (e) of Kammern-Grubgraben (Gilot, 1997; Haesaerts, 1990; Haesaerts *et al.*, 2016; Händel *et al.*, 2021a). All radiocarbon dates were recalibrated with IntCal20 (Reimer *et al.*, 2020) using OxCal version 4.4 (Bronk Ramsey, 2009), bars indicate 1 and 2 sigma ranges. For comparison, the pollen assemblages of (Bergsee (Duprat-Oualid *et al.*, 2017) and the soil development in the loess record of Nussloch (g) (Moine *et al.*, 2017) are given as in Stojakowits *et al.* (2021). Lower panels show calcium (Ca^{2+}) as a measure of dust accumulation in Greenland (h) (note the inverse and logarithmic scale) (Mayewski *et al.*, 1997; Rasmussen *et al.*, 2014), $\delta^{18}O$ values (i) (Rasmussen *et al.*, 2014) and temperature derived from $\delta^{15}N$ of entrapped air (j) (Kindler *et al.*, 2014), all from the NGRIP record (Andersen *et al.*, 2004; Rasmussen *et al.*, 2014), reported on the Greenland Ice Core Chronology (GICC05; Andersen *et al.*, 2006). Blue numbers in Ca^{2+} record represent Greenland Interstadials. [Color figure can be viewed at wileyonlinelibrary.com]

assemblage of Krems-Hundssteig considered here (AH 3.21, 3.22, 3.24 and 3.44) predominantly consists of mammoth, reindeer and horse with minor contributions of red deer, woolly rhinoceros, arctic fox, wolf and hare, as well as micromammals. The minimum number of individuals (MNI) for the relevant horizons was 57 (Fladerer and Salcher-Jedrasiak, 2008; Händel, 2017).

During excavations in the 1930s, numerous lithic artefacts and animal remains, including mammoth tusks, were found at the Gravettian site of Krems-Wachtberg 1930 (Einwögerer, 2000; Fladerer, 2001). Although three find layers have been observed during the excavation, the recovered material was not separated. Thus, all samples must be considered as one complex, and radiocarbon ages (33.4–31.0k cal a BP) point to an Early Gravettian occupation more or less contemporaneous with Krems-Wachtberg 2005–2015 (Fig. 2b; Einwögerer *et al.*, 2009; Händel, 2017). The faunal remains comprise mainly mammoth, wolf, red and arctic fox,

wolverine and to a lesser extent, red deer, reindeer, ibex and musk ox (MNI = 28; Fladerer, 2001; Händel, 2017).

The loess records of Krems-Wachtberg 2005–2015 were studied sedimentologically and indicate a climatic deterioation around the MIS 3–MIS 2 transition (Sprafke *et al.*, 2020) as also indicated elsewhere in central Europe (Stojakowits *et al.*, 2021).

Langenlois A (31–29k cal a BP)

The Upper Palaeolithic site Langenlois is located in the area of the former brickyard Kargl in the southeast of the town of Langenlois (Fig. 1). The find locations Langenlois A–C are located on a loess-covered slope exposed to the east and facing towards the river Kamp. Placed in a valley basin, the site is protected to the north by smaller hills and to the southwest by the prominent Gobelsberg elevation. During the first excavations of the site Langenlois A in the early 1960s, one archaeological horizon was identified, which is characterised by different occupational structures. Three adjacent fireplaces, an unevenly developed cultural layer, and various other features, such as workplaces for the fragmentation of bones, suggest a variety of activities. All specimens analysed here originate from the excavation site Langenlois A and date to 30.8–29.2k cal a BP (Fig. 2c; Einwögerer, 2019). The faunal assemblage is dominated by ibex, followed by horse and reindeer plus a few remains of red deer and mammoth (Einwögerer, 2000).

Kammern-Grubgraben (24–20k cal a BP)

At the Kammern-Grubgraben site, Upper Palaeolithic finds were first collected in 1890 (Spöttl, 1890; Obermaier, 1908; Händel *et al.*, 2021a). However, it was not until 1985 that systematic excavations (1985–1990) began in the area of the present excavation site (Brandtner, 1990, 1996; Montet-White, 1988, 1990). During an inventory project in 2013, 23 000 inventory numbers were assigned, which comprise archaeological and zooarchaeological material (Neugebauer-Maresch *et al.*, 2016). A new phase of field investigations began in 2015, which is still ongoing (Händel *et al.*, 2021a).

Kammern-Grubgraben is one of the few stratified LGM sites in central Europe and is located in the south-eastern extension of the Bohemian-Moravian Highlands (Fig. 1; Händel *et al.*, 2021a). It is situated on a gentle loess-covered slope between two hills, the Heiligenstein in the east and the Geißberg in the west. The site is open towards the south, i.e. to the Kamp River valley and the Danube plain and confined towards the northwest by the adjacent Moravian plateau. Given the harsh environmental conditions during the LGM (Maier *et al.*, 2021; Händel *et al.*, 2021a), this geographic setting may have been advantageous for hunter-gatherer communities, given the wind protection and proximity to water. Sedimentological studies at Kammern-Grubgraben indicate a rather monotonous depositional environment during the LGM, dominated by aeolian deposition of silt-sized loess (Reiss *et al.*, 2022).

Beside lithic and organic artefacts, the Kammern-Grubgraben inventory also includes a large number of faunal remains. The faunal assemblage of Kammern-Grubgraben is dominated by reindeer, followed by horse. There are minor contributions of hare, mammoth, bison, red deer, ibex, wolf, brown bear, wolverine, arctic fox, red fox, goose and ground squirrel (MNI = 234; Pfeifer *et al.* accepted). The zooarchaeological material stems from different archaeological layers, which were addressed differently in various excavation campaigns during the long period of research. The samples analysed here originate from both the Brandtner excavation and the excavation led by the team of Montet-White. Therefore, the labelling of the find horizons varies depending on the excavation year. The Montet-White and Brandtner excavations documented five consecutive archaeological layers (AL 1–5) and assigned these to at least five different occupation phases (Haesaerts *et al.*, 2016; Neugebauer-Maresch *et al.*, 2016). However, more recent investigations indicate that former ALs 2–4 probably represent a single main occupation phase, here referred to as AH 2. The earlier AH 3 (probably corresponding to former AL 5) seems to represent a much less intensive occupation, while AH 1 (former AL 1) at least partly contains relocated finds and suggests contributions from different occupational episodes including a younger, potentially Magdalenian, occupation. Radiocarbon ages of faunal remains (bones and teeth) from AH 1 and 2 (resp. AL 1–4) indicate human activity between 23.7 and 19.5k cal a BP (Fig. 2d,e; Haesaerts *et al.*, 2016; Händel *et al.*, 2021a).

Material and methods

Bone material

The find inventories include large numbers of faunal remains, both bones and teeth, of terrestrial animals, including various carnivores (red fox, arctic fox, wolf and wolverine) and numerous herbivores (woolly mammoth, reindeer, red deer, horse, bison, musk ox, woolly rhinoceros, hare, ibex and goose). Bone material was sorted according to stratigraphic aspects and taxonomically identified by K. Pasda for Kammern-Grubgraben and Langenlois. The faunal remains from Krems-Hundssteig 2000–2002 had already been taxonomically identified and documented by Fladerer and Salcher-Jedrasiak (2008) and the Krems-Wachtberg 1930 inventory by Fladerer (2001). To avoid samples with potentially poor collagen preservation, bones with a compact texture were selected preferentially for collagen extraction and subsequent stable isotope analyses.

In most cases, the same species were selected from the inventories to allow for accurate comparisons between species and sites. Whenever possible, different individuals of a species were selected from one site (Table 1). In order to increase the number of species and to obtain as many species as possible for both periods, the food webs of the Early Gravettian sites Krems-Wachtberg 1930 (KW) and Krems-Hundssteig 2000–2002 (HU) have been combined and are discussed as one coherent food web (KW + HU) in comparison to the Early Epigravettian food web of Kammern-Grubgraben (KG). This decision is justified for KW and HU based on spatial proximity (less than 250 m) and identical ^{14}C age range (Fig. 2a,b). In addition, we included the site Langenlois A (LK, 9 km northeast of KW + HU; Fig. 1) in this study because it contains a considerable number of ibexes, which are rare in KW + HU but also common in KG. LK appears to be around 2k years younger than KW + HU, although its age range overlaps with these sites (Fig. 2c).

In the evaluation and discussion, only bone collagen data are considered, as the values of dental collagen can be considerably enriched in ^{15}N compared with bone collagen, which has been confirmed for dental collagen from reindeer (Fizet *et al.*, 1995; Britton, 2010). In addition to bone collagen analyses from KG–AH 2, four samples from KG–AH 1 were analysed, but these results are not included in the discussion, as it cannot be excluded that they originate from a Magdalenian, i.e. post-LGM occupation. Both dental collagen values and samples originating from KG–AH 1 were not further considered but are listed in Supplementary Table S1 for completeness.

Table 1. List of species and analysed material sampled from Krems-Hundssteig 2000–2002, Krems-Wachtberg 1930, Langenlois A and Kammern-Grubgraben with indication of the find layer and the minimum number of individuals (MNI) at the respective sites. The MNI is stated at the beginning of each newly listed taxon. The abbreviation 'n.d.' means 'not determined'.

Study site	Sample ID	Taxon	Skeletal element	Material	Side	Age	Find layer	MNI
Krems-Hundssteig 2000–2002	HU-100/1	hare (*Lepus* sp.)	Cranium	bone	n.d.	n.d.	3.44	2
Krems-Hundssteig 2000–2002	HU-168/3	hare (*Lepus* sp.)	Cranium	bone	n.d.	n.d.	3.44	
Krems-Hundssteig 2000–2002	HU-253/5	hare (*Lepus* sp.)	Mandibula	bone	right	n.d.	3.24	
Krems-Hundssteig 2000–2002	HU-276/5	horse (*Equus* sp.)	Pisiforme	bone	left	n.d.	3.44	3
Krems-Hundssteig 2000–2002	HU-201/15	horse (*Equus* sp.)	Phalanx 2 (med.)	bone	n.d.	n.d.	3.24	
Krems-Hundssteig 2000–2002	HU-33/4	horse (*Equus* sp.)	Maxilla, P2	tooth	left	n.d.	3.21	
Krems-Hundssteig 2000–2002	HU-158/3	ibex (*Capra ibex*)	Metacarpus III/IV	bone	left	n.d.	3.24	1
Krems-Hundssteig 2000–2002	HU-159/2	arctic fox (*Vulpes lagopus*)	Mandibula	bone	left	n.d.	3.44	1
Krems-Hundssteig 2000–2002	HU-165/1	red deer (*Cervus elaphus*)	Calcaneus	bone	n.d.	n.d.	3.44	2
Krems-Hundssteig 2000–2002	HU-372/24	red deer (*Cervus elaphus*)	Mandibula	bone	n.d.	n.d.	3.22	
Krems-Hundssteig 2000–2002	HU-206/2,3	red deer (*Cervus elaphus*)	Carpale	bone	n.d.	n.d.	3.24	
Krems-Hundssteig 2000–2002	HU-156/2	red fox (*Vulpes vulpes*)	Cranium	bone	n.d.	n.d.	3.44	2
Krems-Hundssteig 2000–2002	HU-432/1	red fox (*Vulpes vulpes*)	Cranium, P4 and M1	tooth	n.d.	n.d.	3.23	
Krems-Hundssteig 2000–2002	HU-196/3	reindeer (*Rangifer tarandus*)	Radius	bone	left	n.d.	3.24	2
Krems-Hundssteig 2000–2002	HU-69/6	reindeer (*Rangifer tarandus*)	Femur	bone	left	n.d.	3.21	
Krems-Hundssteig 2000–2002	HU-211/2	reindeer (*Rangifer tarandus*)	Calcaneus	bone	left	n.d.	3.24	
Krems-Hundssteig 2000–2002	HU-210/9	reindeer (*Rangifer tarandus*)	Astragalus	bone	left	n.d.	3.24	
Krems-Hundssteig 2000–2002	HU-272/5	wolf (*Canis lupus*)	Metatarsus IV	bone	right	n.d.	3.24	1
Krems-Hundssteig 2000–2002	HU-190/11	woolly mammoth (*Mammuthus primigenius*)	Astragalus	bone	right	subadult	3.24	5
Krems-Hundssteig 2000–2002	HU-192/17	woolly mammoth (*Mammuthus primigenius*)	Astragalus	bone	right	subadult	3.24	
Krems-Hundssteig 2000–2002	HU-103/18	woolly mammoth (*Mammuthus primigenius*)	Astragalus	bone	right	subadult	3.24	
Krems-Hundssteig 2000–2002	HU-198/1	woolly mammoth (*Mammuthus primigenius*)	Astragalus	bone	right	subadult	3.24	
Krems-Hundssteig 2000–2002	HU-184/27	woolly mammoth (*Mammuthus primigenius*)	Carpale 3	bone	right	n.d.	3.24	
Krems-Hundssteig 2000-2002	HU-192/6	woolly mammoth (*Mammuthus primigenius*)	Phalanx	bone	n.d.	infantile	3.24	
Krems-Hundssteig 2000–2002	HU-181/6	woolly mammoth (*Mammuthus primigenius*)	Capitatum	bone	left	n.d.	3.24	
Krems-Hundssteig 2000–2002	HU-408/1	woolly rhinoceros (*Coelodonta antiquitatis*)	Phalanx 3 (dist.), vestigial	bone	n.d.	n.d.	3.23	2
Krems-Hundssteig 2000–2002	HU-348/9	woolly rhinoceros (*Coelodonta antiquitatis*)	Vertebra thoracalis	bone	n.d.	juvenile/ subadult	3.22	
Krems-Wachtberg 1930	KW-MK 923	hare (*Lepus* sp.)	Pelvis	bone	n.d.	n.d.	n.d.	1
Krems-Wachtberg 1930	KW-MK 928	hare (*Lepus* sp.)	Metapodium	bone	n.d.	n.d.	n.d.	
Krems-Wachtberg 1930	KW-MK 1070	horse (*Equus* sp.)	Long bones	bone	n.d.	n.d.	n.d.	1
Krems-Wachtberg 1930	KW-MK 1105	ibex (*Capra ibex*)	Humerus	bone	n.d.	n.d.	n.d.	1
Krems-Wachtberg 1930	KW-MK 917	muskox (*Ovibos moschatus*)	Phalanx 1, proximal	bone	n.d.	n.d.	n.d.	1
Krems-Wachtberg 1930	KW-MK 931	arctic fox (*Vulpes lagopus*)	Ulna	bone	left	n.d.	n.d.	1
Krems-Wachtberg 1930	KW-MK 935	arctic fox (*Vulpes lagopus*)	Mandibula	bone	left	n.d.	n.d.	
Krems-Wachtberg 1930	KW-MK 936	arctic fox (*Vulpes lagopus*)	Humerus	bone	left	n.d.	n.d.	
Krems-Wachtberg 1930	KW-MK 932	red fox (*Vulpes vulpes*)	Mandibula	bone	right	n.d.	n.d.	3
Krems-Wachtberg 1930	KW-MK 933	red fox (*Vulpes vulpes*)	Mandibula	bone	right	n.d.	n.d.	
Krems-Wachtberg 1930	KW-MK 934	red fox (*Vulpes vulpes*)	Mandibula	bone	right	n.d.	n.d.	
Krems-Wachtberg 1930	KW-MK 938	red fox (*Vulpes vulpes*)	Radius	bone	right	n.d.	n.d.	
Krems-Wachtberg 1930	KW-MK 1008	reindeer (*Rangifer tarandus*)	Radius (prox.)	bone	n.d.	n.d.	n.d.	1
Krems-Wachtberg 1930	KW-MK 907	wolf (*Canis lupus*)	Manibula	bone	left	adult	n.d.	5
Krems-Wachtberg 1930	KW-MK 908	wolf (*Canis lupus*)	Manibula	bone	left	adult	n.d.	
Krems-Wachtberg 1930	KW-MK 909	wolf (*Canis lupus*)	Manibula	bone	left	adult	n.d.	

(*Continued*)

Table 1. (*Continued*)

Study site	Sample ID	Taxon	Skeletal element	Material	Side	Age	Find layer	MNI
Krems-Wachtberg 1930	KW-MK 910	wolf (*Canis lupus*)	Manibula	bone	left	adult	n.d.	
Krems-Wachtberg 1930	KW-MK 911	wolf (*Canis lupus*)	Manibula	bone	left	adult	n.d.	
Krems-Wachtberg 1930	KW-MK 976	wolverine (*Gulo gulo*)	Mandibula	bone	right	adult	n.d.	3
Krems-Wachtberg 1930	KW-MK 974	wolverine (*Gulo gulo*)	Mandibula	bone	right	adult	n.d.	
Krems-Wachtberg 1930	KW-MK 975	wolverine (*Gulo gulo*)	Mandibula	bone	right	adult	n.d.	
Krems-Wachtberg 1930	KW-MK 1045	woolly mammoth (*Mammuthus primigenius*)	Long bones	bone	n.d.	n.d.	n.d.	3
Krems-Wachtberg 1930	KW-MK 1034	woolly mammoth (*Mammuthus primigenius*)	Femur	bone	right	n.d.	n.d.	
Krems-Wachtberg 1930	KW-MK 1033	woolly mammoth (*Mammuthus primigenius*)	Femur	bone	left	juvenile	n.d.	
Krems-Wachtberg 1930	KW-MK 1104	woolly mammoth (*Mammuthus primigenius*)	Femur	bone	right	n.d.	n.d.	
Krems-Wachtberg 1930	KW-MK 1107	woolly rhinoceros (*Coelodonta antiquitatis*)	Humerus	bone	n.d.	n.d.	n.d.	1
Langenlois A	LK-F1/1076	hare (*Lepus* sp.)	Scapula	bone	left	adult	n.d.	2
Langenlois A	LK-1209/DI	hare (*Lepus* sp.)	Pelvis	bone	left	juvenile	n.d.	
Langenlois A	LK-B3/159	goose (*Anser* sp.)	Ulna, proximal	bone	right	adult	n.d.	1
Langenlois A	LK-A5-B5/43	horse (*Equus* sp.)	Radius	bone	right	adult	n.d.	2
Langenlois A	LK-1572	horse (*Equus* sp.)	Radius	bone	right	n.d.	n.d.	
Langenlois A	LK-D3/368	ibex (*Capra ibex*)	Metacarpus	bone	right	adult	n.d.	5
Langenlois A	LK-E3/611	ibex (*Capra ibex*)	Metacarpus	bone	right	adult	n.d.	
Langenlois A	LK-D1/1212	ibex (*Capra ibex*)	Metacarpus	bone	right	adult	n.d.	
Langenlois A	LK-D3/369	ibex (*Capra ibex*)	Metacarpus	bone	right	adult	n.d.	
Langenlois A	LK-G1/799	ibex (*Capra ibex*)	Radius, distial	bone	left	juvenile	n.d.	
Langenlois A	LK-E3/625	red deer (*Cervus elaphus*)	Mandibula, I3	bone	right	adult	n.d.	1
Langenlois A	LK-Rt-1	reindeer (*Rangifer tarandus*)	Os centroquartale	bone	left	n.d.	n.d.	2
Langenlois A	LK-Rt-2	reindeer (*Rangifer tarandus*)	Metatarsus, proximal	bone	left?	n.d.	n.d.	
Kammern-Grubgraben	KG 240	hare (*Lepus* sp.)	Mandibula	bone	right	adult	3	1
Kammern-Grubgraben	KG 627	hare (*Lepus* sp.)	Humerus	bone	right	adult	3	
Kammern-Grubgraben	KG 241	hare (*Lepus* sp.)	Metatarsus III	bone	right	adult	3	
Kammern-Grubgraben	KG 2542	hare (*Lepus* sp.)	Tibia, distal	bone	left	adult	3	
Kammern-Grubgraben	KG 2331	hare (*Lepus* sp.)	Calcaneus	bone	left	adult	3	
Kammern-Grubgraben	KG 1500	hare (*Lepus* sp.)	Tibia	bone	n.d.	adult	3	
Kammern-Grubgraben	KG 76	hare (*Lepus* sp.)	Humerus	bone	left	adult	3	
Kammern-Grubgraben	KG 1024	hare (*Lepus* sp.)	Tibia	bone	right	n.d.	3	
Kammern-Grubgraben	KG 1061	hare (*Lepus* sp.)	Calcaneus	bone	right	adult	3	
Kammern-Grubgraben	KG 872	hare (*Lepus* sp.)	Tibia	bone	left	adult	3	
Kammern-Grubgraben	KG 711	hare (*Lepus* sp.)	Mandibula	bone	left	adult	3	
Kammern-Grubgraben	KG 225	hare (*Lepus* sp.)	Radius	bone	left	adult	3	
Kammern-Grubgraben	KG 391	bison (*Bison* sp.)	Metatarsus III + IV	bone	n.d.	adult	4	1
Kammern-Grubgraben	KG 1155	bison (*Bison* sp.)	Mandibula, I1	tooth	right	adult	3	
Kammern-Grubgraben	KG 2652	bison (*Bison* sp.)	Mandibula, Processus muscularis	bone	left	adult	3 or 4	
Kammern-Grubgraben	KG 2547	bison (*Bison* sp.)	Maxilla, Molar	tooth	n.d.	n.d.	2 or 3	
Kammern-Grubgraben	KG 754	brown bear (*Ursus arctos*)	Mandibula, I3	tooth	right	adult	3	1
Kammern-Grubgraben	KG 2672	goose (*Anser* sp.)	Ulna	bone	n.d.	adult	3	1
Kammern-Grubgraben	KG 5	horse (*Equus* sp.)	Mandibula, Molar	tooth	n.d.	adult	3	4
Kammern-Grubgraben	KG 10	horse (*Equus* sp.)	Metatarsus III	bone	right?	adult	1	
Kammern-Grubgraben	KG 44	horse (*Equus* sp.)	Os tarsi centrale	bone	left	adult	3	
Kammern-Grubgraben	KG 384	horse (*Equus* sp.)	Mandibula	bone	right	adult	2	

(*Continued*)

Table 1. (*Continued*)

Study site	Sample ID	Taxon	Skeletal element	Material	Side	Age	Find layer	MNI
Kammern-Grubgraben	KG 14	horse (*Equus* sp.)	Maxilla	bone	right	adult	3	
Kammern-Grubgraben	KG 1282	horse (*Equus* sp.)	Phalanx 1 anterior or posterior	bone	n.d.	adult	3	
Kammern-Grubgraben	KG 1324	horse (*Equus* sp.)	Metatarsus III	bone	n.d.	adult	3	
Kammern-Grubgraben	KG 1017	horse (*Equus* sp.)	Metacarpus III	bone	n.d.	adult	2	
Kammern-Grubgraben	KG 1944	horse (*Equus* sp.)	Humerus	bone	right	infantile	3	
Kammern-Grubgraben	KG 955	horse (*Equus* sp.)	Maxilla	bone	right	adult	3	
Kammern-Grubgraben	KG 956	horse (*Equus* sp.)	Maxilla	bone	right	adult	3	
Kammern-Grubgraben	KG 912	horse (*Equus* sp.)	Maxilla	bone	right	adult	3	
Kammern-Grubgraben	KG 97	ibex (*Capra ibex*)	Phalanx 2 anterior or posterior	bone	n.d.	adult	4	3
Kammern-Grubgraben	KG 214	ibex (*Capra ibex*)	Phalanx 2 anterior or posterior	bone	n.d.	adult	3	
Kammern-Grubgraben	KG 385	ibex (*Capra ibex*)	Tibia	bone	right	adult	3	
Kammern-Grubgraben	KG 1288	ibex (*Capra ibex*)	Phalanx 2, posterior	bone	n.d.	adult	4	
Kammern-Grubgraben	KG 149	ibex (*Capra ibex*)	Mandibula	bone	right	infantile	3	
Kammern-Grubgraben	KG 249	ibex (*Capra ibex*)	Mandibula	bone	right	adult	3	
Kammern-Grubgraben	KG 1286	ibex (*Capra ibex*)	Phalanx 2, posterior	bone	n.d.	adult	3	
Kammern-Grubgraben	KG 1277	ibex (*Capra ibex*)	Phalanx 2, posterior	bone	n.d.	adult	3	
Kammern-Grubgraben	KG 1613	ibex (*Capra ibex*)	Phalanx 2 anterior or posterior	bone	n.d.	infantile	1	
Kammern-Grubgraben	KG 454	ibex (*Capra ibex*)	Mandibula	bone	right	adult	3	
Kammern-Grubgraben	KG 1491	arctic fox (*Vulpes lagopus*)	Mandibula	bone	right	adult	3	2
Kammern-Grubgraben	KG 1485	arctic fox (*Vulpes lagopus*)	Mandibula	bone	left	adult	3	
Kammern-Grubgraben	KG 223	arctic fox (*Vulpes lagopus*)	Caninus	bone	left	adult	3	
Kammern-Grubgraben	KG 1488	arctic fox (*Vulpes lagopus*)	Cranium, M1 and M2	tooth	right	adult	3	
Kammern-Grubgraben	KG 2069	arctic fox (*Vulpes lagopus*)	Mandibula	bone	right	adult	3	
Kammern-Grubgraben	KG 804	red deer (*Cervus elaphus*)	Phalanx 2 anterior or posterior	bone	n.d.	adult	3	1
Kammern-Grubgraben	KG 826	red deer (*Cervus elaphus*)	Mandibula, M2	tooth	left	adult	3	
Kammern-Grubgraben	KG 2606	red deer (*Cervus elaphus*)	Metatarsus, proximal	bone	left	adult	3	
Kammern-Grubgraben	KG 1949	red deer (*Cervus elaphus*)	Maxilla, C	tooth	n.d.	n.d.	3	
Kammern-Grubgraben	KG 239	red fox (*Vulpes vulpes*)	Maxilla	bone	left	adult	3	1
Kammern-Grubgraben	KG 1	reindeer (*Rangifer tarandus*)	Antlers	antlers	n.d.	adult	3	8
Kammern-Grubgraben	KG 3	reindeer (*Rangifer tarandus*)	Humerus	bone	right	juvenile/ subadult	3	
Kammern-Grubgraben	KG 4	reindeer (*Rangifer tarandus*)	Antlers	antlers	n.d.	adult	3	
Kammern-Grubgraben	KG 6	reindeer (*Rangifer tarandus*)	Mandibula	bone	right	adult	3	
Kammern-Grubgraben	KG 7	reindeer (*Rangifer tarandus*)	Mandibula	bone	left	adult	3	
Kammern-Grubgraben	KG 8	reindeer (*Rangifer tarandus*)	Metatarsus III + IV	bone	right	adult	3	
Kammern-Grubgraben	KG 165	reindeer (*Rangifer tarandus*)	Mandibula	bone	right	subadult	3	
Kammern-Grubgraben	KG 261	reindeer (*Rangifer tarandus*)	Mandibula	bone	left	subadult	3	
Kammern-Grubgraben	KG 319	reindeer (*Rangifer tarandus*)	Humerus	bone	right	adult	3	
Kammern-Grubgraben	KG 327	reindeer (*Rangifer tarandus*)	Mandibula	bone	right	adult	3	
Kammern-Grubgraben	KG 375	reindeer (*Rangifer tarandus*)	Talus/Astragalus	bone	left	adult	1	
Kammern-Grubgraben	KG 376	reindeer (*Rangifer tarandus*)	Metatarsus III + IV	bone	n.d.	adult	4	
Kammern-Grubgraben	KG 377	reindeer (*Rangifer tarandus*)	Os centroquartale	bone	right	adult	1	
Kammern-Grubgraben	KG 378	reindeer (*Rangifer tarandus*)	Metatarsus III + IV	bone	n.d.	adult	4	
Kammern-Grubgraben	KG 379	reindeer (*Rangifer tarandus*)	Radius	bone	left	adult	3	
Kammern-Grubgraben	KG 163	reindeer (*Rangifer tarandus*)	Mandibula	bone	left	infantile	4	

(*Continued*)

Table 1. (*Continued*)

Study site	Sample ID	Taxon	Skeletal element	Material	Side	Age	Find layer	MNI
Kammern-Grubgraben	KG 173	reindeer (*Rangifer tarandus*)	Mandibula	bone	right	adult	3	
Kammern-Grubgraben	KG 172	reindeer (*Rangifer tarandus*)	Mandibula	bone	right	adult	3	
Kammern-Grubgraben	KG 1618	reindeer (*Rangifer tarandus*)	Mandibula	bone	right	adult	2	
Kammern-Grubgraben	KG 1612	reindeer (*Rangifer tarandus*)	Mandibula	bone	right	juvenile	4	
Kammern-Grubgraben	KG 394	reindeer (*Rangifer tarandus*) (m.)	Antlers	antlers	n.d.	adult	3	
Kammern-Grubgraben	KG 174	reindeer (*Rangifer tarandus*) (m.)	Mandibula	bone	right	juvenile	4	
Kammern-Grubgraben	KG 1063	wolf (*Canis lupus*)	Maxilla	bone	left	n.d.	3	1
Kammern-Grubgraben	KG 646	wolf (*Canis lupus*)	Mandibula, P4	tooth	left	adult	4	
Kammern-Grubgraben	KG 2622	wolf (*Canis lupus*)	Mandibula, I3	bone	left	adult	3	
Kammern-Grubgraben	KG 361	wolf (*Canis lupus*) or brown bear (*Ursus arctos*)	Mandibula, I3	tooth	left	n.d.	4	
Kammern-Grubgraben	KG 1590	wolverine (*Gulo gulo*) (m.)	Mandibula	bone	left	adult	3	1
Kammern-Grubgraben	KG 2113	woolly mammoth (*Mammuthus primigenius*)	Long bones	bone	n.d.	n.d.	3	1
Kammern-Grubgraben	KG 2	woolly mammoth (*Mammuthus primigenius*)	Long bones	bone	n.d.	adult	3	
Kammern-Grubgraben	KG 38	woolly mammoth (*Mammuthus primigenius*)	Long bones	bone	n.d.	adult	3	
Kammern-Grubgraben	KG 1109	woolly mammoth (*Mammuthus primigenius*)	Tibia	bone	n.d.	adult	3	
Kammern-Grubgraben	KG 1110	woolly mammoth (*Mammuthus primigenius*)	Long bones	bone	n.d.	adult	3	
Kammern-Grubgraben	KG 1111	woolly mammoth (*Mammuthus primigenius*)	Radius	bone	right	adult	3	
Kammern-Grubgraben	KG 1113	woolly mammoth (*Mammuthus primigenius*)	Long bones	bone	n.d.	adult	3	

Fourier-transform infrared (FTIR) spectroscopy

FTIR spectroscopy was used as a pre-screening method on a defined set of samples (KG: $n = 7$, HU: $n = 4$, KW: $n = 4$, LK: $n = 3$) of bone powder to detect the preservation of collagen (Cersoy *et al.*, 2016; Lebon *et al.*, 2016). It was further applied on the respective extracts to check for the chemical purity of bone collagen. Less than 2 mg of each powdered sample was used for FTIR spectroscopy in attenuated total reflectance mode (IR Prestige-21, Shimadzu). The device parameters were set according to the method of Lebon *et al.* (2016). Infrared spectra were obtained from 64 scans per run with a spectral resolution of $2\,cm^{-1}$ in the wavenumber range of $4000–370\,cm^{-1}$. To account for sample heterogeneity and to determine instrumental reproducibility, each sample was measured in triplicate. Prior to every sample measurement, a new baseline (air, CO_2) was set. Wavenumbers in the range of $1710–1590\,cm^{-1}$ and $1110–940\,cm^{-1}$ represent the amide I band and the $_{v3}$phosphate ($_{v3}PO_4$)-band, respectively (Lambert *et al.*, 1998; Lebon *et al.*, 2016).

Collagen extraction

Collagen extraction followed a slightly modified version of the method of Bocherens *et al.* (1991). About 0.5–2.0 g was carefully sawn from each animal bone using a rotary tool (Proxxon-Micromot, Germany) with a circular diamond blade. Wherever necessary, samples were cleaned with sandpaper and a common toothbrush before soaking them in deionised water for 30 min. Samples that were hardened or glued for preservation were additionally soaked in acetone to remove varnish from the bones.

Subsequently, samples were ultrasonically cleaned in deionised water for 10 s and dried in a drying oven at 40°C overnight. Samples were then ground using a mortar and pestle. 0.25–1.0 g of each powdered sample (0.3–0.7 mm grain size) was weighed in centrifuge tubes and soaked in 1 M HCl to dissolve minerals, while samples were shaken on a rotator for 20 min. Subsequently, the samples were repeatedly washed with distilled water and centrifuged (Heraeus Multifuge 3L-R, Thermo Electron Corporation, USA) at 3000 rpm for 5 min, until a pH of 6 was reached. For dissolution of humic acids, the pellets were soused with 0.125 M NaOH and left under the fume hood for 20 h. Thereafter, all samples were washed again with distilled water and centrifuged until pH was neutral. In the next step, the pellets were soaked in 0.01 M HCl (pH 2) and incubated for 10–17 h in a water bath (Julabo, SW23, Germany) at 95°C to solubilise the gelatine.

Finally, the dissolved gelatine was filtrated through MF-Millipore membrane filters (5.0 µm) using vacuum flasks and filter funnels, frozen and lyophilised.

Stable isotope analysis

Samples were analysed in duplicate or triplicate at the stable isotope laboratories at Forschungszentrum Jülich (FZJ) and Friedrich-Alexander-Universität Erlangen-Nürnberg (FAU), respectively. Some 240–260 µg of collagen was wrapped in tin capsules and combusted in an elemental analyser (Flash2000, Thermo Fisher, USA, FZJ; NC 2500, Carlo Erba, Italy, FAU) and measured online with a coupled isotope ratio mass spectrometer (DeltaV plus, Thermo Fisher, USA, FZJ; DeltaPlus, Thermo-Finnigan, Germany, FAU). Carbon and nitrogen measurements were performed within one analysis run on the same sample.

Isotope results are reported as delta (δ) values per mille (‰) according to the equation:

$$\delta = R_S/R_{St} - 1. \quad (1)$$

R_S is the isotope ratio ($^{13}C/^{12}C$, $^{15}N/^{14}N$) of the sample and R_{St} of the respective standard. δ values are normalised to the VPDB (Vienna Pee Dee Belemnite) scale for carbon and the AIR (atmospheric nitrogen) scale for nitrogen (Coplen 2011).

The calibration of laboratory standards and scale-normalisation of $\delta^{13}C$ raw values was based upon the International Atomic Energy Agency (IAEA) reference standards IAEA-CH6 ($\delta^{13}C = -10.45‰$) and IAEA-CH7 ($\delta^{13}C = -32.15‰$), and the United States Geological Survey (USGS) standard USGS24 ($\delta^{13}C = -16.05‰$). The average standard deviation of replicate measurements for $\delta^{13}C$ standards measured in the respective runs was 0.24‰ for IAEA-CH7 ($n = 8$), and 0.10‰ for the laboratory standard peptone ($n = 8$).

Calibration of laboratory standards and scale-normalisation of $\delta^{15}N$ raw values is based upon the international reference standards IAEA-N-2 ($\delta^{15}N = 20.3‰$), IAEA-N-1 ($\delta^{15}N = 0.4‰$) and USGS25 ($\delta^{15}N = -30.4‰$). The average standard deviation of replicate measurements of $\delta^{15}N$ standards measured in the respective runs was 0.28‰ for IAEA-N-1 ($n = 8$), 0.15‰ for IAEA-N-2 ($n = 8$) and 0.14‰ for lab standard peptone ($n = 8$). Samples were also analysed for their weight percentage carbon (%) and nitrogen (%) using elemental standards for calibration. The measurement error of the element concentrations was <5%. Elemental content and atomic C/N ratios were used to check for chemical purity.

Quality criteria for collagen preservation

Impurities or diagenesis may lead to a shift in the isotope values of prehistoric bone collagen. The C/N ratio is known to be a quality criterion for collagen and was used to validate collagen purity (Guiry and Szpak, 2021). Reported C/N ratios for pure collagen vary between 2.9 and 4.0 (DeNiro, 1985; Grupe *et al.*, 2003; Coltrain *et al.*, 2004; Bösl *et al.*, 2006; Hoke *et al.*, 2019), but samples with C/N > 3.6 should be rejected as the collagen purity for those cannot be guaranteed (Ambrose, 1990; van Klinken, 1999).

Another quality criterion used was collagen yield and element content. According to DeNiro and Weiner (1988), the minimum yield of extracted collagen (wt.%) should be 2%, but more recent studies suggest 1% (Ambrose, 1990, Ambrose and Norr, 1993; Dobberstein *et al.*, 2009) or even 0.5% (van Klinken, 1999) as sufficient for acceptable preservation (Hoke *et al.*, 2019). The nitrogen and carbon content of unaltered collagen is 11–16 wt.% and 35 ± 9 wt.%, respectively, (van Klinken, 1999) and was used as additional criteria for the quality of the extracted collagen.

Statistics

Statistical calculations were carried out with R studio (version R-4.2.2). Shapiro–Wilk tests were used to check for normal distribution of data. Possible outliers were determined using Grubb's tests. Wilcoxon–Mann–Whitney tests were carried out to test the null hypothesis of whether two groups are statistically indifferent (Dytham, 2011). For all analyses performed, a significance level of 0.05 was chosen.

Comparisons of isotopic niches among different animal communities were analysed using the Stable Isotope Bayesian Ellipses in R (SIBER) package (Jackson *et al.*, 2011). It must be emphasised here that isotopic niches do not necessarily correspond to ecological niches, since, for example, different trophic niches can lead to the same isotopic ranges (Jackson *et al.*, 2011). In comparison to simple convex-hull methods, SIBER is based on multivariate ellipse metrics, with the advantage of being independent of sample size while enabling robust comparison between data sets of different sizes (Jackson *et al.*, 2011).

We calculated convex hulls, i.e. total area and standard ellipse area (SEA, in ‰²) of herbivorous taxa represented by more than three data points. For the KW + HU and KG food webs, these include horse, hare, reindeer and woolly mammoth, for LK and KG, ibex. The SEA explains 40% of all potential specimens that fit into the respective niches, based on a Bayesian probability estimation. The SEA is sensitive to sample size, which is why we used the recommended standard ellipse area corrected for sample size (SEAc) (Jackson *et al.*, 2011).

Results

Preservation and purity of collagen

FTIR spectra revealed a sufficient amount of collagen in all powdered bone samples analysed (Fig. 3a). The FTIR spectra of the powdered untreated samples show a distinct peak in the amide I band range (1710–1590 cm^{-1}) indicative for collagen, while the $_{v3}PO_4$ band range (1110–940 cm^{-1}), indicative for bone phosphate (PO_4), is obviously more pronounced.

Collagen quality was confirmed by FTIR spectra of the extracted collagen of selected samples (Fig. 3b). After collagen extraction, no $_{v3}PO_4$ band could be detected anymore, indicating complete dissolution of $_{v3}PO_4$ during the collagen extraction procedure. Instead, the amide band is most pronounced, indicating that pure collagen was extracted.

Collagen yields (wt.%), varied between 0.8 and 16% and were on average 4.3% at KG and 7.0% at KW. Two samples (woolly mammoth 'KG 1110' and ibex 'KG 249') yielded collagen content <0.5%. However, other chemical characteristics, such as %N, %C and C/N ratios of these samples, are still within the acceptable range for well-preserved collagen, except for KW-MK-938 (red fox), KG-2652 (bison) and KG-1500 (hare), which all had nitrogen and carbon content that were too low (Table S1). All other samples are thus considered reliable in terms of collagen preservation and are included in the further evaluation. The high purity of all the extracted collagen samples was generally confirmed by their C/N ratios which range between 2.9 and 3.6 as expected for pure collagen (Table S1).

Isotopic results of bone collagen

All stable isotope results are shown in $\delta^{15}N$ vs. $\delta^{13}C$ plots separated for the Early Gravettian/pre-LGM sites KW + HU (Fig. 4a), the Early Gravettian/pre-LGM site LK (Fig. 4b) and the Early Epigravettian/LGM site KG (Fig. 4c). Shapiro–Wilk tests confirm a normal distribution of the complete dataset ($\delta^{15}N$: $W = 0.97455$, $p < 0.05$ and $\delta^{13}C$: $W = 0.9042$, $p < 0.05$). We excluded one outlier (hare 'WA-MK 923', confirmed by Grubb's test) from further evaluations and listed it only in Supplementary Table S1, as the exceptionally low $\delta^{13}C$ values most likely indicate modern contamination.

In the pre-LGM food web of KW + HU, all common herbivorous species except mammoth exhibit mean $\delta^{15}N$ values between 2.1 ± 1.2 (hare) and 5.3 ± 2.3‰ (woolly rhinoceros). Musk ox also exhibits a very high $\delta^{15}N$ value of 7.7‰. However, they are represented by only one specimen and therefore may not be representative. As mentioned, mammoths exhibit considerably higher $\delta^{15}N$ values than other herbivores, with a mean value of 8.2 ± 0.8‰ and are thus almost on the same level as the carnivorous species wolf and wolverine that exhibit $\delta^{15}N$ mean values of 8.8 ± 0.7 and 8.8 ± 1.1‰, respectively (Fig. 4a). Arctic fox and red fox show

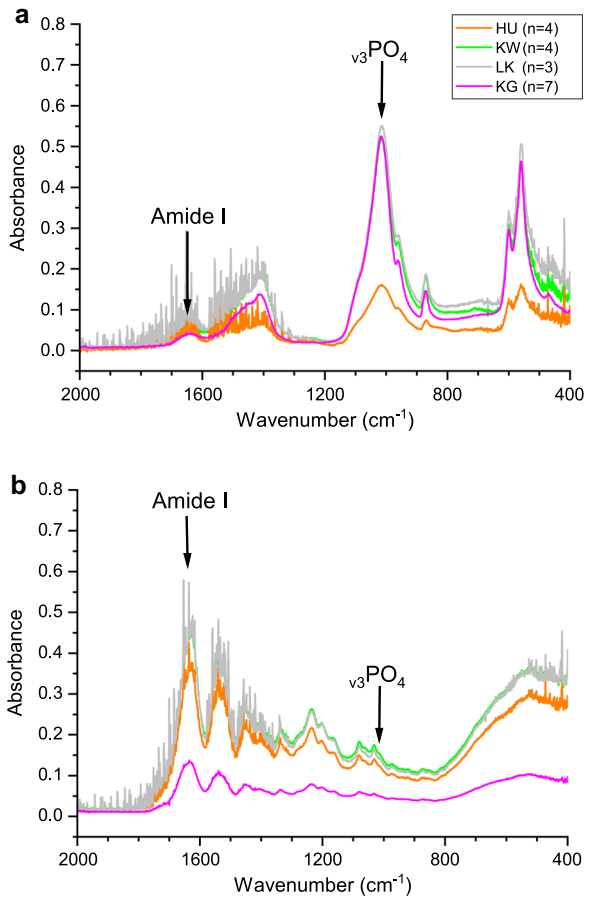

Figure 3. FTIR spectra of (a) bone powder and (b) extracted bone collagen of the same samples from HU, KW, LK and KG, respectively. Note that the *y*-axis is arbitrary. [Color figure can be viewed at wileyonlinelibrary.com]

slightly lower $\delta^{15}N$ mean values of 7.5 ± 1.2 and 7.2 ± 0.4‰, respectively.

In the pre-LGM food web of LK, hare exhibits a mean $\delta^{15}N$ value of 3.6 ± 0.1‰, reindeer of 4.7 ± 3.9‰, horse of 3.5 ± 0.9‰ and ibex of 4.7 ± 0.7‰. Single specimens of red deer and goose exhibited $\delta^{15}N$ values of 2.8 and 7.0‰ (Fig. 4b).

At the LGM site KG, $\delta^{15}N$ mean values of herbivore taxa range from 1.8 ± 0.7 in hare to 3.9‰ in goose, which is again represented by only one specimen (Fig. 4c). The highest single values of herbivores belong to infantile individuals of ibex and horse (3.6‰ and 3.5‰, respectively). In contrast to the pre-LGM sites, the $\delta^{15}N$ values of mammoth (2.5 ± 0.9‰) at KG are in the range of other herbivores. Carnivores show $\delta^{15}N$ mean values of 7.5 ± 2.4‰ and are thus 5.2‰ higher than herbivores. However, the arctic fox's $\delta^{15}N$ values are highest but exhibit a large scatter (8.6 ± 3.2‰), while wolf (7.3 ± 1.9‰), red fox (6.7‰) and wolverine (5.9‰) show lower values.

A comparison between pre-LGM (KW + HU, LK) and LGM (KG) isotope-derived food webs shows similarities but also some differences. The main similarity between both periods is a separation between two clusters of herbivores: in KW + HU and KG, horse and hare have generally lower $\delta^{13}C$ values than the cluster formed by ibex and reindeer (Fig. 4a,c). In LK the data on hare, reindeer and horse are too small to draw such a conclusion. Red deer exhibits a varying position in $\delta^{15}N$ vs. $\delta^{13}C$ space: in the pre-LGM period at KW + HU it falls between the fields of rhinoceros and horse on the one side, and hare on the other (Fig. 4a), while in the LGM it plots together with reindeer and ibex (Fig. 4c). The most striking

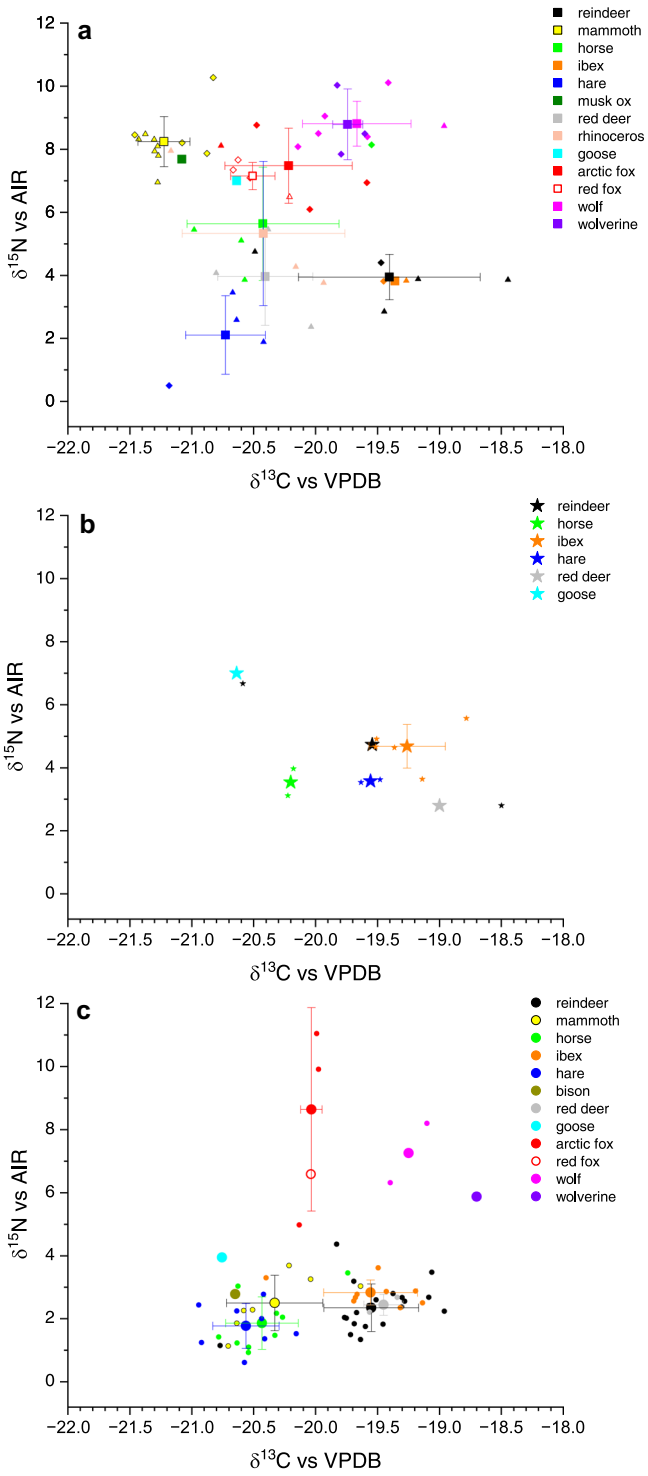

Figure 4. $\delta^{13}C$ and $\delta^{15}N$ bone collagen values of (a) Early Gravettian/pre-LGM sites KW + HU (33–31k cal a BP), (b) Early Gravettian/pre-LGM site LK (31–29k cal a BP) and (c) Early Epigravettian/LGM site KG (24–20k cal a BP). Mean values are represented as big squares in (a) for KW + HU, as big stars in (b) for LK, and as big circles in (c) for KG. Whiskers represent the respective standard deviations. Small symbols indicate values of the respective study site, with triangles = HU, diamonds = KW, stars = LK and circles = KG. [Color figure can be viewed at wileyonlinelibrary.com]

difference between pre-LGM (KW + HU) and LGM (KG) is, however, the shift of the mammoth cluster mainly related to the strong $\delta^{15}N$ decrease between both periods as already mentioned above. During the pre-LGM period, the cluster of mammoths does not match any of the herbivores except a single musk ox and rhinoceros bone, while the data cluster overlaps with those of horse and hare in the LGM.

For better evaluation, we statistically tested the isotopic differences between pre-LGM and LGM sites for the most common herbivorous taxa, i.e. mammoth, horse, hare, reindeer and ibex using the Wilcoxon–Mann–Whitney test (Fig. 5a,b). All tested pairs belonged to KW + HU versus KG, except for ibex, for which LK versus KG was used. With the exception of hare, all taxa had significantly higher δ^{15}N values in the pre-LGM than in the LGM (Fig. 5a).

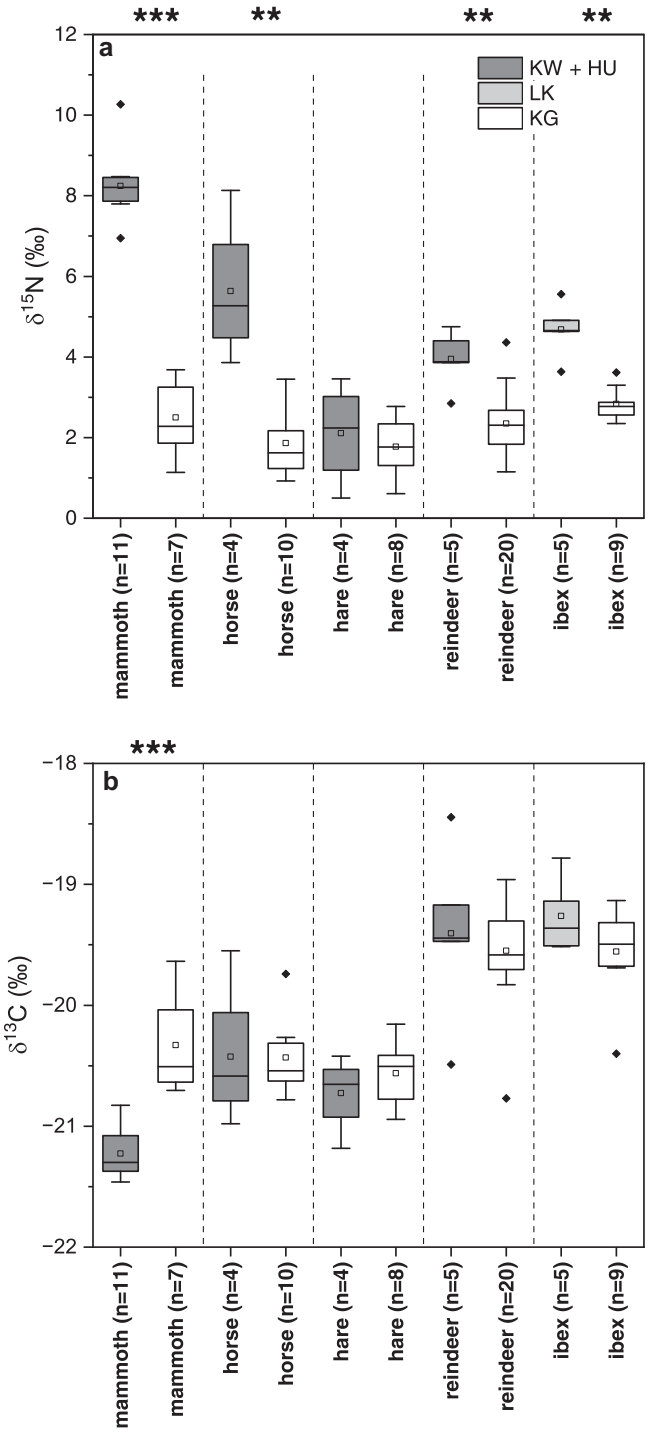

Figure 5. Box plots of most common herbivore δ^{15}N (a) and δ^{13}C (b) values of KW + HU (dark grey) and LK (light grey) in comparison with KG (white). Only taxa with $n > 3$ are shown. Boxes represent 25 and 75 percentiles, open squares means, horizontal lines medians, whiskers standard deviations and black diamonds outliers. Stars indicate probability values that the null hypothesis ('values in both time periods are not different') can be rejected (***$p < 0.001$, **$0.001 < p < 0.01$, *$0.01 < p < 0.05$).

In terms of absolute values, a marked δ^{15}N shift occurs between both periods except for hare. In the pre-LGM period, δ^{15}N mean values of all herbivores are on average 3.3‰ higher than in the LGM food web. If mammoth is excluded, the shift is still 2.0‰.

Detailed statistical analyses demonstrate that only the δ^{13}C of mammoth is significantly different between both periods and exhibits the lowest δ^{13}C values in the pre-LGM period of KW + HU (Fig. 5b). In KW + HU, δ^{13}C mean values of herbivores range from -21.2 ± 0.2‰ in mammoth to -19.4 ± 0.7‰ in reindeer, showing a slightly broader range compared with the LGM (−20.8 in goose to -19.6 ± 0.4‰ in reindeer). The largest δ^{13}C shift between both periods occurs in mammoths: from -21.2 ± 0.2‰ in the pre-LGM period to -20.3 ± 0.4‰ in the LGM. Wolf and wolverine in KW + HU exhibit δ^{13}C mean values of -19.7 ± 0.4 and -19.7 ± 0.1‰, while arctic fox and red fox show slightly lower δ^{13}C mean values of -20.2 ± 0.4 and -20.5 ± 0.2‰, respectively. In the LGM, carnivores exhibit δ^{13}C mean values ranging from -20.0 ± 0.1‰ in arctic fox to −18.7‰ in wolverine (Fig. 4a).

In comparison to the LGM, the results of SIBER analyses for the pre-LGM confirm larger isotopic niche widths for all analysed herbivores but mammoth. Mammoth has a SEAc of 0.6‰² in the pre-LGM (KW + HU) compared with 0.9‰² in the LGM. The SEAc of the other pre-LGM herbivores range from 0.9 (ibex, LK) to 3.1‰² (horse, KW + HU), while in the LGM the same species have SEAc of 0.5 and 0.7‰², respectively (Fig. 6). When considering the isotopic niche areas of both periods, the isotopic niche of ibex is the least variable. Horse shows the largest isotopic niche in the pre-LGM and the biggest change in isotopic niche width between pre-LGM and LGM (Fig. 6).

Discussion

Herbivore niche partitioning indicated by δ^{13}C

Niche partitioning can generally reflect a spatial separation in terms of different habitats, distinct dietary habits, temporal variation, or even temporal and spatial avoidance (Kronfeld-Schor *et al.*, 2001; Stewart *et al.*, 2003; Britton *et al.*, 2012; Bocherens *et al.*, 2015). Herbivore data in the pre-LGM period show a larger variability and thus partly broader isotopic niches in the SIBER analysis than during the LGM (Fig. 6a). This is best explained by the climatic deterioration that significantly affected the environment and consequently the stable isotope pattern of herbivores (Zimov *et al.*, 2012; Drucker *et al.*, 2018; Drucker, 2022).

In comparison to the δ^{15}N values, the δ^{13}C clustering of herbivores (with the exception of mammoth) is relatively stable over time (Fig. 5b) and can be directly linked to their dietary habits, which are determined by the regional plant communities, except for migratory mammals. The δ^{13}C results point to two main groups of herbivores: horse and hare show lower, and reindeer and ibex higher δ^{13}C values (Fig. 5b). Mammoth belongs to the first group during the LGM but has lower δ^{13}C values than all other taxa in the pre-LGM (Fig. 5b). In (modern) arctic environments, various plant groups show different isotopic compositions (Nadelhoffer *et al.*, 1996; Stevens and Hedges, 2004). Modern plant communities from different arctic locations include grasses, sedges, forbs, shrubs, mosses, fungi and lichen differing significantly in both δ^{15}N and δ^{13}C values (Barnett, 1994; Wang and Wooller, 2006; Munizzi, 2017; Drucker, 2022). Forbs, graminoids and fungi show the highest δ^{15}N values. Shrubs, forbs and graminoids (grasses and sedges) exhibit the lowest δ^{13}C values, while lichen shows the highest

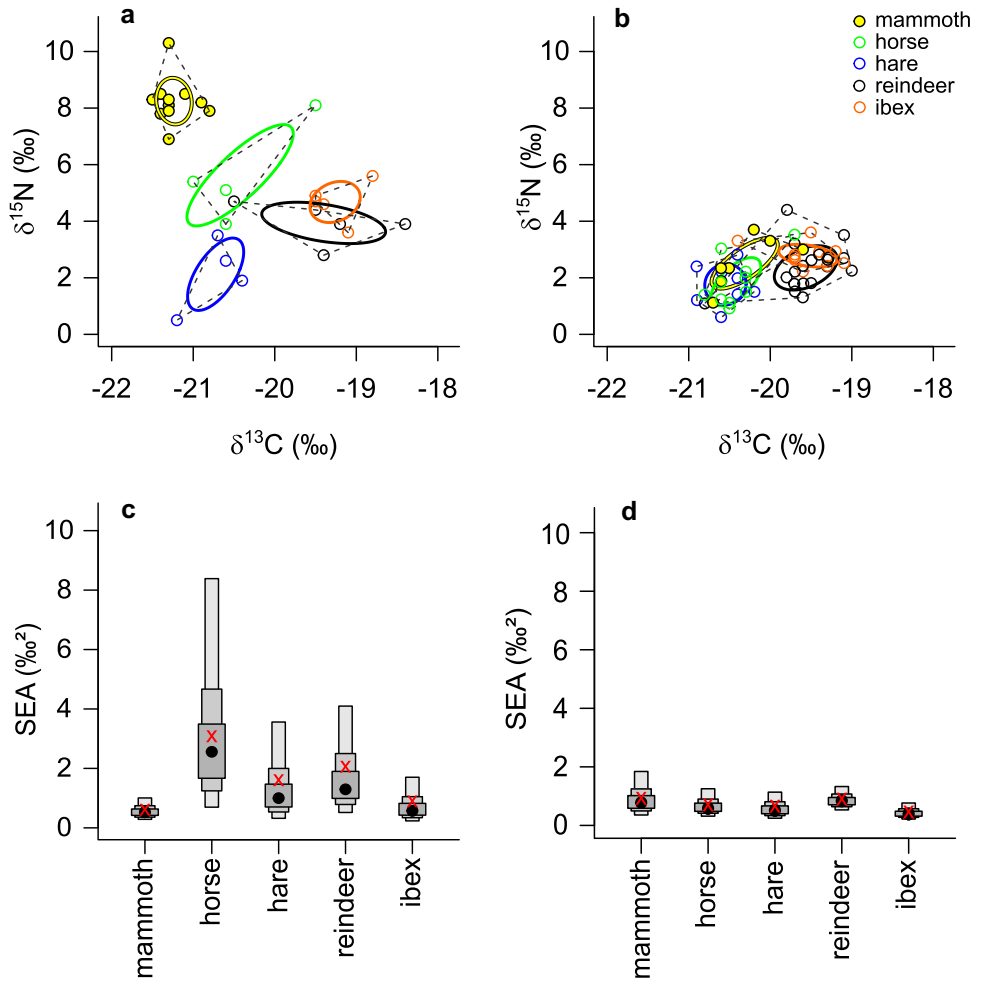

Figure 6. Standard ellipse areas (SEA) (solid ellipses) and convex hulls (dashed lines) of different herbivores from (a) Early Gravettian/pre-LGM food webs KW + HU and LK (ibex) (33–29k cal a BP) and (b) Epigravettian/LGM food web KG (24–20k cal a BP). Lower panels are density plots of SEA of (c) Early Gravettian/pre-LGM food webs KW + HU and LK (ibex), and (d) Epigravettian/LGM food web KG. Black circles are mode values of the SEAb values, i.e. SEA calculated using a Bayesian approach. Grey boxes represent 50, 75 and 95% credibility. Red crosses are SEA values corrected for sample size. For the number of specimens, see Fig. 5. [Color figure can be viewed at wileyonlinelibrary.com]

$\delta^{13}C$ values (Fizet *et al.*, 1995; Finstad and Kielland, 2011). In times when other food sources are deficient, reindeer are thought to consume high proportions of lichen, which explains their high $\delta^{13}C$ values (Fizet *et al.*, 1995; Drucker *et al.*, 2001; Bocherens, 2003; Stevens *et al.*, 2008; Finstad and Kielland, 2011; Bocherens *et al.*, 2015). Consequently, previous observations of high $\delta^{13}C$ values n fossil reindeer bones at various locations, such as Belgium (Bocherens *et al.*, 2001; Germonpré *et al.*, 2009), Germany (Stevens *et al.*, 2009; Drucker *et al.*, 2011), France (Fizet *et al.*, 1995; Drucker *et al.*, 2000, 2003; Bocherens, 2003; Drucker and Henry-Gambier, 2005; Bocherens *et al.*, 2005, 2011; Drucker, 2022) or Beringia, i.e. Siberia (Iacumin *et al.*, 2000) and Alaska-Yukon (Fox-Dobbs *et al.*, 2008), were explained by a high proportion of lichen consumption. As ibex falls into the cluster of reindeer, a diet similar to that of reindeer could also be considered for ibex during the glacial, although nowadays the diet of European *Capra ibex* consists mainly of graminoids (Parrini *et al.*, 2009). However, it is known that the Siberian ibex (*Capra sibirica*) in the Altai Mountains preferentially feeds on lichens (Fedosenko and Blank, 2001).

The observed dietary $\delta^{13}C$ differences are probably related to different habitats. As carbon isotope fractionation is driven by distinct pathways of photosynthesis, C_3 and C_4 plants can be easily distinguished by their $\delta^{13}C$ values (Farquhar *et al.*, 1989). However, the presence of substantial amounts of C_4 plants in the investigated region during the last glacial can be excluded (Iacumin *et al.*, 1997; Bocherens, 2003; Stojakowits *et al.*, 2020, 2021). Rather, a range of environmental factors, such as humidity, temperature and atmospheric CO_2 partial pressure affected the carbon isotope composition of the prevalent C_3 vegetation at that time, which directly affected physiological parameters controlling isotope fractionation in plant tissues (Tieszen, 1991). Decreased temperatures, a lower atmospheric CO_2 partial pressure, and increased water stress provoke increased $\delta^{13}C$ values, while high water availability, reduced light, and denser vegetation result in overall decreased $\delta^{13}C$ values (Tieszen, 1991; Pataki *et al.*, 2003; Drucker *et al.*, 2008; Kohn, 2010; Bonafini *et al.*, 2013). Apart from increased lichen consumption, elevated $\delta^{13}C$ values could therefore be a response either to increasing drought or to reduced vegetation cover, as exemplified for fossil reindeer (Drucker *et al.*, 2011).

On a landscape scale, different soil moisture conditions on slope versus valley positions result in distinct $\delta^{13}C$ differences. For instance, C_3 plants growing in valleys had on average 2‰ lower $\delta^{13}C$ values than those on the slopes in an arid landscape in northwest China (Wang *et al.*, 2005). Such small-scale differences are relevant for the local (e.g. hare) or likely non-migratory (e.g. bison, horse, ibex) mammals in our assemblage, while reindeer (Britton, 2010) and mammoth (Wooller *et al.*, 2021) presumably migrated over greater distances and could therefore also reflect the isotopic signatures of a broader geographical range. However, it is a matter of debate whether reindeer migration took place in Europe in every region and at every time during the last glacial

period (Fontana, 2017). For the investigated area, it can therefore be assumed that at least ibex lived in a habitat characterised by edaphically drier conditions which might have been the case on the exposed slopes and higher elevations north and northwest of the study sites (Fig. 1). In contrast, hare, horse and bison presumably lived in habitats with edaphically more humid conditions, e.g. in valleys or on the floodplains of the Danube and its tributaries south of the study sites (Fig. 1). At least for modern wild Przewalski's horses, a preference for riparian habitats in the Gobi Desert is confirmed by satellite telemetry. In contrast to Asiatic wild asses in the same region, Przewalski's horses have a much smaller home range along riparian zones, and prefer floodplain vegetation (Kaczensky *et al.*, 2008). In addition, horses and bison need to drink water regularly (Caboń-Raczyńska *et al.*, 1983, 1987; Scheibe *et al.*, 1998; Kaczensky *et al.*, 2008). These arguments support an edaphically more humid, most likely riparian habitat, where hares and bison lived alongside horses during the LGM (Fig. 4b). Whether the $\delta^{13}C$ values of potentially migratory species, such as reindeer and mammoth, just accidentally fall within the fields of mammals of edaphically drier (ibex) and wetter habitats (horse, hare, bison), respectively, remains to be resolved with other techniques (e.g. $^{87}Sr/^{86}Sr$; Britton *et al.*, 2011) in the future.

Schwartz-Narbonne *et al.* (2015) reported that certain ecological niches can be occupied by multiple species, and despite the rather inhospitable conditions during the last glacial, these environments apparently allowed for a greater variety of habitats with options for for food sources for both generalists and specialists. For instance, the authors report an overlap of equine $\delta^{15}N$ values with those of woolly mammoth, whereas in our study, horse, hare and reindeer of the pre-LGM food web overlap but at the same time have broader niches than in the LGM (Fig. 6a,c), suggesting availability of more diverse food sources for these taxa during pre-LGM. This is confirmed by the pollen record from Bergsee in the Black Forest (southern Germany), which is one of the few continuous records of floral biodiversity covering the LGM in the northern Alpine foreland (Fig. 2f; Duprat-Oualid *et al.*, 2017). During the time of KW, HU and LK, i.e. in the latest MIS 3, the Bergsee record still shows up to 30% shrub and tree pollen, whereas the values decrease to below 20% in the LGM. This is in agreement with other palynological records that indicate small patches of trees during late MIS 3, while after 30k cal a BP arctic plant assemblages prevailed and pedogenesis came to an end (Stojakowits *et al.*, 2021). The presence of shrubs and trees in the study area during the pre-LGM is evidenced by an abundance of charcoal found in the archaeological layers at KW + HU (Neugebauer-Maresch and Cichocki, 2008; Händel, 2017). Wood anatomical studies on charcoal particles from KW + HU and the adjacent site Krems-Wachtberg 2005–2015 allowed the identification of predominantly pine wood with minor contributions of spruce/larch and single specimens of fir and beech wood (Einwögerer, 2000; Neugebauer-Maresch and Cichocki 2008; Cichocki *et al.*, 2014).

In both periods, goose exhibits a particularly high nitrogen isotope value among the herbivores, possibly reflecting an occupation of a particular habitat that differs from that of other herbivores. This could be connected to the uptake of a higher proportion of aquatic food or partial feeding in more southerly habitats due to seasonal migration. An accurate interpretation, however, is hardly possible due to the scarce data.

Food resources and trophic levels

$\delta^{15}N$ values of the most abundant herbivores during the pre-LGM show a large inter-taxon variability (Fig. 5a) leading to a broad niche partitioning (Fig. 6a). In contrast, niche breadth shrinks considerably during the LGM and isotopic niches cluster closer together (Fig. 6a). Most likely this is the result of a narrower range of food resources during the cold and arid LGM compared with the climatically more favourable previous periods.

Apart from hare, the $\delta^{15}N$ values for all other common herbivore taxa decrease towards the LGM (Fig. 5a). Several previous studies have already documented such a $\delta^{15}N$ shift at around the same time for horse, reindeer, bison or red deer (Drucker *et al.*, 2003; Richards and Hedges, 2003; Stevens and Hedges, 2004; Stevens *et al.*, 2008). Our data allow further narrowing of the time frame for the $\delta^{15}N$ shift to a period approximately between 29 and 24k cal a BP for Lower Austria.

At the pre-LGM sites KW + HU, $\delta^{15}N$ values of all carnivores are on average 2.8‰ higher than those of the herbivores, whereas during the LGM, the average difference between carnivores and herbivores is 5.2‰, suggesting a difference of at least one trophic level and increased trophic enrichment in the LGM. In the $\delta^{13}C$–$\delta^{15}N$ space, two clusters of carnivores are observed at KW + HU (Fig. 4a): wolf and wolverine ($\delta^{13}C = -19.7$‰, $\delta^{15}N = 8.8$‰ for both) exhibit 0.5‰ higher $\delta^{13}C$ and about 1.1‰ higher $\delta^{15}N$ values than arctic and red fox ($\delta^{13}C = -20.2$‰ and $\delta^{13}C = -20.5$‰, $\delta^{15}N = 7.50$‰ and $\delta^{15}N = 7.2$‰, respectively). Assuming a trophic enrichment factor of 1.1 ± 1.1‰ for $\delta^{13}C$ and 3.2 ± 1.8‰ for $\delta^{15}N$ (Krajcarz *et al.*, 2018), prey isotope values for fox result in the range of all common herbivores except ibex, reindeer and mammoth. This may suggest that foxes at KW + HU fed mainly on carrion and small mammals like hare. Likewise, wolf and wolverine could have fed on all abundant herbivores except for hare and ibex. This is not in conflict with a previous study that inferred horses and possibly mammoth as prey items for Pleistocene wolves based on statistical analyses (Bocherens *et al.*, 2015).

However, our dataset is biased by prehistoric humans' selection and therefore lacks certain species, e.g. micromammals that may have been an important prey item especially for foxes (Baumann *et al.*, 2020). Red and arctic foxes are opportunistic predators that can change trophic behaviour and adapt to a new diet whenever necessary (Baumann *et al.*, 2020). Foraging on micromammals on the one hand and scavenging on large mammals (potentially even other carnivores) on the other could explain the high $\delta^{15}N$ variability of arctic fox in the LGM. In foxes, it has been observed that specialisation on micromammal prey or carrion of large herbivores also leads to inter-specimen $\delta^{15}N$ differences of up to several per mill at other Palaeolithic sites (Baumann *et al.*, 2020), similar as in the LGM at KG.

The special case of woolly mammoth

In some cases, altering environmental conditions may lead to changing isotopic niches of certain species, such as the woolly mammoth. In the pre-LGM food web, mammoths reveal the highest $\delta^{15}N$ values of all herbivores and appear on a similar level as carnivores. This phenomenon is already known from other pre-LGM sites in Eurasia, e.g. from France (Bocherens *et al.*, 2005; Drucker *et al.*, 2015), north-eastern China (Ma *et al.*, 2017, 2021), Belgium (Bocherens *et al.*, 1997, 2001), Beringia (Bocherens *et al.*, 1994; Fox-Dobbs *et al.*, 2008), Germany (Bocherens *et al.*, 2011; Drucker *et al.*, 2015) and Yakutia (Bocherens *et al.*, 1996; Szpak *et al.*, 2010; Iacumin *et al.*, 2000, 2010). These high $\delta^{15}N$ values in mammoth collagen could indicate a special diet and thus a distinct dietary niche, a particular habitat, or mammoth-specific physiological or metabolic processes. Results from compound specific isotope

analyses on collagen amino acids (phenyl-alanine and glutamate) of Pleistocene mammoths from Yukon, Canada, showed, however, that the high $\delta^{15}N$ values of collagen come from high $\delta^{15}N$ values of the plants consumed rather than from metabolic processes (Schwartz-Narbonne *et al.*, 2015; Naito *et al.*, 2016). Several studies show that mammoths mainly fed on forbs and graminoids, i.e. grasses and sedges, which tend to have higher $\delta^{15}N$ values (Stewart *et al.*, 2003; Wang and Wooller, 2006) compared with shrubs and lichen (Wang and Wooller, 2006; Finstad and Kielland, 2011; Kristensen *et al.*, 2011). Moreover, remains of grasses and sedges were also found in the jaws of fossil mammoths from Beringia (Guthrie, 2001; Drucker, 2022). A similar diet can also be reconstructed for woolly rhinoceros and steppe bison, which show $\delta^{15}N$ values partly similar to those of mammoths in the pre-LGM food web in our study (Fig. 4a) and may suggest a special dietary niche. In addition, the high $\delta^{15}N$ values in combination with the low $\delta^{13}C$ values of pre-LGM mammoth collagen could also indicate a freshwater plant food source. Kirillova *et al.* (2016) found considerable amounts of freshwater plants in MIS 3 mammoth faeces from northern Russia and concluded that mammoths may also have occupied freshwater, riparian and watershed biotopes.

Our pre-LGM data imply that mammoths occupied an ecological niche where high $\delta^{15}N$ values and lower $\delta^{13}C$ values were prevalent and that was not used by other herbivores to the same extent. $\delta^{15}N$ values of plants are controlled by inorganic primary nitrogen sources (NO_3^-, NH_4^+ and N_2) in the soil as well as their respective isotope discrimination, caused by incorporation or dissimilation (Högberg, 1997; Evans, 2001; Werner and Schmidt, 2002). In addition, great amounts of mammoth dung may have functioned as organic fertiliser in soils which would have resulted in higher $\delta^{15}N$ values of plants (Georgi *et al.*, 2005; Bogaard *et al.*, 2007; Fraser *et al.*, 2011) in the preferred ecological habitat of mammoths during pre-LGM time. This interpretation, however, seems very unlikely for our dataset, as other herbivores do not show elevated $\delta^{15}N$ values.

Accordingly, ecological patterns of mammoth in the pre-LGM period support both distinct feeding habits and the occupation of a specific habitat that is entirely different from habitats of other herbivores (the exception in our study sample is a single musk ox and rhinoceros specimen) (Figs. 4, 5). Changing climate in different geographical or temporal zones towards the end of the Pleistocene, however, may have led to the disappearance of such special niches and specific adaptations of mammoth populations (Drucker *et al.*, 2003; Schwartz-Narbonne *et al.*, 2015). This is in accordance with Nadachowski *et al.* (2018) who reported significant changes in mammoth territories across Europe between 29 and 14 ka and an almost complete disappearance of mammoths during the LGM around 21–19 ka for the North European Plain. Drucker *et al.* (2018) show that the distinct ecological niche of the woolly mammoth changed shortly after the LGM in Europe around 18k cal a BP. $\delta^{15}N$ values of mammoths from Mezhyrich in the Eastern European Plain decreased to the level of other herbivorous species and are in accordance with the mammoth nitrogen isotope values from Kammern-Grubgraben in this study (Figs. 4, 5). Based on our data, however, the decline of mammoth $\delta^{15}N$ values already occurred around 22k cal a BP and thus earlier than previously reported. One possible cause for these changes is the climatic deterioration of the LGM that started around 30k cal a BP and caused large-scale climatic and environmental changes on both global and regional scales (Luetscher *et al.*, 2015; Kämpf *et al.*, 2022). Alternatively, pre-LGM mammoths could have spent most of the time in other regions with distinctly higher isotope values of food sources and just seasonally migrated into the study area. As a consequence, the pre-LGM mammoths may have been more migratory than mammoths during the LGM.

Implications for environmental changes between the pre-LGM and the LGM

In general, substantial environmental changes may lead to changes in the nitrogen isotope pattern at the base of terrestrial food webs (Stevens *et al.*, 2008; Bocherens *et al.*, 2014; Schwartz-Narbonne *et al.*, 2015). This is evident in our study, where mean $\delta^{15}N$ values for herbivores are generally lower in the LGM than the pre-LGM periods, except for hare (Fig. 5a). Plant $\delta^{15}N$ values depend on various factors, such as soil $\delta^{15}N$, pedogenesis, nutrient availability, soil acidity and nitrogen cycling (Högberg, 1997; Drucker *et al.*, 2003; Stevens and Hedges, 2004; Stevens *et al.*, 2008). These parameters are to a great extent controlled by climate factors, which is why plant and soil $\delta^{15}N$ values indirectly correlate with climatic factors, such as mean annual precipitation and mean annual temperature (Handley *et al.*, 1999; Amundson *et al.*, 2003, Craine *et al.*, 2015). The $\delta^{15}N$ values of modern soils show a latitudinal variability, where cold and/or wet ecosystems at high latitudes are the most depleted and hot and/or arid zones the most ^{15}N enriched (Amundson *et al.*, 2003). However, $\delta^{15}N$ values of animal collagen in the last glacial may also have been influenced by temperature-induced thawing of permafrost affecting soil moisture and soil activity (Stevens *et al.*, 2008). On the other hand, low temperatures hamper nitrogen cycling processes such as remineralisation, nitrification and denitrification leading to lower $\delta^{15}N$ values (Drucker *et al.*, 2003). Results similar to ours were reported by Stevens *et al.* (2008), who found significant changes in $\delta^{15}N$ collagen of reindeer over the last glacial period. Before 24k cal a BP, reindeer had significantly higher $\delta^{15}N$ values (mean: 4.2‰) than after 24k cal a BP, when $\delta^{15}N$ values gradually decreased (mean: 2.9‰) until 16k cal a BP when, finally, $\delta^{15}N$ slightly increased again as conditions became wetter (Stevens *et al.*, 2008). Higher $\delta^{15}N$ values in our study (Figs. 4, 5) would thus correspond to higher soil moisture and increased soil microbial activity before the LGM when compared with the LGM.

The pre-LGM sites fall into a time period with severe climatic fluctuations best known from Greenland ice core records (Fig. 2h,i,j). For instance, $\delta^{15}N$ values of air enclosed in bubbles and $\delta^{18}O$ values from ice cores of the North Greenland Ice Core Project (NGRIP) provide temperature records and are inversely correlated with Ca^{2+} records representing dust deposition (Mayewski *et al.*, 1997; Andersen *et al.*, 2004; Kindler *et al.*, 2014; Rasmussen *et al.*, 2014). The pre-LGM sites were occupied around the short-termed Greenland Interstadials 5.2 and 5.1, during which seasonal melting of continuous permafrost may have occurred. As such, a predominance of tundra gley soils has been reported for this time interval in the loess–palaeosol sequence of the Nussloch site in southern Germany (Fig. 2g; Antoine *et al.*, 2009; Moine *et al.*, 2017; Maier *et al.*, 2021). At Krems-Wachtberg 2005–2015, the sediment sequence of this time interval partly shows periglacial features (Terhorst *et al.*, 2014), which was also confirmed for the main archaeological layer AH 4 (Händel *et al.*, 2021b). The slightly broader range of $\delta^{13}C$ values of bone collagen from this time period may also indicate an ameliorated climate, as it reflects a more diversified diet in a mosaic environment. This is in agreement with pollen data from the Alpine region and the Black Forest showing a predominance of forest–tundra vegetation for this time interval

in contrast to the subsequent period of the LGM (Heiri *et al.*, 2014; Stojakowits *et al.*, 2021; Kämpf *et al.*, 2022).

Considering the $\delta^{15}N$ value shift as an indication of environmental and climatic changes, decreased $\delta^{15}N$ collagen values from the LGM site KG would accordingly correspond to cold and arid conditions as continuous permafrost prevailed and large amounts of water were stored in permafrost soils and adjacent glaciated areas (Stevens *et al.*, 2008). Low temperatures but relatively stable conditions can be deduced from the NGRIP record (Fig. 2h,i,j), and loess records from KG point to relatively constant environmental conditions during the main occupation phase (Reiss *et al.*, 2022). Low soil moisture, hardly any soil activity and only incipient tundra gley formation in the predominantly homogeneous loess (Antoine *et al.*, 2009) are assumed for the period between 21 and 19 ka (Maier *et al.*, 2021). Moreover, Drucker *et al.* (2012) attributed lower $\delta^{15}N$ collagen values of reindeer, red deer and horse to continuous permafrost and/or to the proximity of glacier fields, and the highest $\delta^{15}N$ collagen values to regions of discontinuous permafrost.

Conclusions

We compared $\delta^{13}C$ and $\delta^{15}N$ of faunal collagen from the Early Gravettian/pre-LGM sites HU, KW and LK with the Early Epigravettian/LGM site KG (AH 2). Food webs from both periods reveal a characteristic structure with differences in trophic ecology between herbivores and carnivores. A $\delta^{13}C$ clustering between the herbivorous species hare and horse on the one hand and ibex on the other hand points to niche partitioning among herbivorous groups associated with distinct habitats along a local humidity gradient. During the pre-LGM period, the potentially migratory mammoth does not cluster in one of these groups, but in the LGM it overlaps with hare, horse and bison. Reindeer, on the other hand, clusters with ibex in both periods, albeit being considered as migratory. These ambiguities related to the migratory behaviour of mammoth and reindeer can only be resolved by applying other isotope techniques such as $^{87}Sr/^{86}Sr$ in future studies.

The general $\delta^{15}N$ shift of 3.3‰ between all herbivores of two investigated time periods (KW + HU, KG) can be attributed to climatically induced changes in the environment. This shift lowers to 2.0‰ if mammoth is excluded. Previously reported, strikingly high nitrogen isotope values of mammoths can also be confirmed for the Early Gravettian/pre-LGM sites in this study, but at the same time, we show that the disappearance of this particular niche occurred during the LGM before 23–22k cal a BP, and thus earlier than previously established for central Europe. The isotopic niche widths expressed by SIBER analyses indicate larger habitat diversity for herbivores during the pre-LGM compared with the LGM, with the exception of ibex and mammoth. Accordingly, the herbivore clusters tend to increasingly overlap at the LGM site KG. As climatic conditions became more extreme in the course of the LGM, and woody plants declined, certain habitats disappeared and different species had to share ecological niches. This decrease in habitats should also have resulted in a greater homogeneity of food sources as indicated by restricted isotopic ranges of non-migratory herbivores during the LGM compared with the pre-LGM period. Also, with the advances of Alpine and Baltic ice shields during the LGM, the ranges for migratory mammals, in particular mammoth, most probably became more restricted, which might have led to a greater isotopic similarity to more local mammals during the LGM.

Acknowledgements. We gratefully acknowledge financial support from the German Research Foundation (DFG) (grant no. MA 4235/12-1, project no. 424736737). We thank U. Simon and N. Buchinger for discussion about the site Kammern-Grubgraben. We thank N. Bova, T. Stauber and J. Bügenburg for assistance in the isotope laboratory, C. Ehli for help with FTIR-analyses in the facility of the Institute of Physical Chemistry (FAU) and M. Häusser for support with GIS. We thank K. Britton and an anonymous reviewer for their thorough reviews and A. Brauer for editorial work. Open Access funding enabled and organized by Projekt DEAL.

Competing interests

The authors have declared that no competing interests exist.

Data availability statement

All relevant data are available in Table 1 and Supplementary Table S1.

Author contributions—LR carried out collagen extractions, evaluated and visualised the data and wrote the original draft. CM, MH, AL, AM and KP contributed substantially to the text. KP taxonomically identified the study material from Kammern-Grubgraben and Langenlois A. HW carried out most of the stable isotope analyses. TE and MH provided the study material. All authors reviewed and approved the manuscript. CM and KP initially designed the study with contributions from AM and TE.

Supporting information

Additional supporting information can be found in the online version of this article.

Supplementary Table S1. Isotopic and chemical results of the analysed material. A single measurement was carried out for sample HU-348/9. The abbreviation 'n.d.' means 'not determined'. The absolute difference (AD) between individual measured values of a single sample is given for samples measured in duplicate ($n = 2$). Standard deviations (SDs) are given for all other samples measured in triplicate ($n = 3$). At the bottom of the table, samples are listed that were not used in the evaluation (tooth samples, samples from AH 1/AL 1, and outliers as defined in the text). For rows labelled with 'X', values are missing.

Abbreviations. LGM, Last Glacial Maximum; pre-LGM, pre-Last Glacial Maximum; k cal a BP, calibrated kiloyears before present; SIBER, Stable Isotope Bayesian Ellipses in R; MIS, Marine Isotope Stage; AH, archaeological horizon; MNI, minimum number of individuals; AL, archaeological layer; KW, Krems-Wachtberg; HU, Krems-Hundssteig; LK, Langenlois A; KG, Kammern-Grubgraben; FTIR, Fourier-transform infrared; ATR, attenuated total reflectance; °C, degree Celsius; CO_2, carbon dioxide; g, gram; M, Molar; HCl, hydrochloric acid; NaOH, sodium hydroxide; $_{v3}PO_4$, $_{v3}$phosphate; FZJ, Forschungszentrum Jülich; FAU, Friedrich-Alexander-Universität Erlangen-Nürnberg; δ, delta; ‰, per mill; %, percent; C, carbon; N, nitrogen; VPDB, Vienna Pee Dee Belemnite; IAEA, International Atomic Energy Agency; USGS, United States Geological Survey; wt.%, weight percentage; TA, Total Area; SEA, Standard Ellipse Area; SEAc, Standard Ellipse Area corrected for sample size; PO_4, phosphate; Sr, strontium; NO_3^-, nitrate; NH_4^+, ammonium; N_2, atomic nitrogen; NGRIP, North Greenland Ice Core Project; GI, Greenland Interstadial.

References

Ambrose, S.H. (1990) Preparation and characterization of bone and tooth collagen for isotopic analysis. *Journal of Archaeological Science*, 17, 431–451.

Ambrose, S.H. & Norr, L. (1993) Experimental evidence for the relationship of the carbon isotope ratios of whole diet and dietary protein to those of bone collagen and carbonate. In: Lambert, J. & Grupe, G. (Eds.) *Prehistoric Human Bone, Archaeology at the Molecular Level*. Berlin, Heidelberg: Springer. pp. 1–37.

Amundson, R., Austin, A.T., Schuur, E.A.G., Yoo, K., Matzek, V., Kendall, C. et al. (2003) Global patterns of the isotopic composition of soil and plant nitrogen. *Global Biogeochemical Cycles*, 17, 1031.

Andersen, K.K., Azuma, N., Barnola, J.-M., Bigler, M., Biscaye, P., Caillon, N., et al. (2004) High-resolution record of Northern Hemisphere climate extending into the last interglacial period. *Nature*, 431, 147–151.

Andersen, K.K., Svensson, A., Johnsen, S.J., Rasmussen, S.O., Bigler, M., Röthlisberger, R. et al. (2006) The Greenland Ice Core Chronology 2005, 15–42 ka. Part 1: constructing the time scale. *Quaternary Science Reviews*, 25, 3246–3257.

Antoine, P., Rousseau, D.D., Moine, O., Kunesch, S., Hatté, C., Lang, A. et al. (2009) Rapid and cyclic aeolian deposition during the Last Glacial in European loess: a high-resolution record from Nussloch, Germany. *Quaternary Science Reviews*, 28, 2955–2973.

Barnett, B.A. (1994). Carbon and nitrogen isotope ratios of caribou tissue, vascular plants, and lichens from northern Alaska. Master's Thesis, University of Alaska, Fairbanks.

Baumann, C., Bocherens, H., Drucker, D.G. & Conard, N.J. (2020) Fox dietary ecology as a tracer of human impact on Pleistocene ecosystems. *PLoS One*, 15, e0235692. Available at: https://doi.org/10.1371/journal.pone.0235692

Blaser, P.C., Kipfer, R., Loosli, H.H., Walraevens, K., van Camp, M. & Aeschbach-Hertig, W. (2010) A 40 ka record of temperature and permafrost conditions in northwestern Europe from noble gases in the Ledo-Paniselian Aquifer (Belgium). *Journal of Quaternary Science*, 25(6), 1038–1044.

Bocherens, H. (2003) Isotopic biogeochemistry and the palaeoecology of the mammoth steppe fauna. *Deinsea*, 9(1), 57–76.

Bocherens, H., Billiou, D., Patou-Mathis, M., Bonjean, D., Otte, M. & Mariotti, A. (1997) Paleobiological implications of the isotopic signatures (^{13}C,^{15}N) of fossil mammal collagen in Scladina Cave (Sclayn, Belgium). *Quaternary Research*, 48, 370–380.

Bocherens, H. & Drucker, D. (2003) Trophic level isotopic enrichment of carbon and nitrogen in bone collagen: case studies from recent and ancient terrestrial ecosystems. *International Journal of Osteoarchaeology*, 13, 46–53.

Bocherens, H., Drucker, D.G., Billiou, D., Patou-Mathis, M. & Vandermeersch, B. (2005) Isotopic evidence for diet and subsistence pattern of the Saint-Césaire I Neanderthal: review and use of a multi-source mixing model. *Journal of Human Evolution*, 49, 71–87.

Bocherens, H., Drucker, D.G., Bonjean, D., Bridault, A., Conard, N.J., Cupillard, C. et al. (2011) Isotopic evidence for dietary ecology of cave lion (*Panthera spelaea*) in North-Western Europe: prey choice, competition and implications for extinction. *Quaternary International*, 245, 249–261.

Bocherens, H., Drucker, D.G., Germonpré, M., Lázničková-Galetová, M., Naito, Y.I., Wissing, C. et al. (2015) Reconstruction of the Gravettian food-web at Předmostí I using multi-isotopic tracking ^{13}C, ^{15}N, ^{34}S of bone collagen. *Quaternary International*, 359-360, 211–228.

Bocherens, H., Drucker, D.G. & Madelaine, S. (2014) Evidence for a ^{15}N positive excursion in terrestrial foodwebs at the Middle to Upper Palaeolithic transition in south-western France: implications for early modern human palaeodiet and palaeoenvironment. *Journal of Human Evolution*, 69, 31–43.

Bocherens, H., Fizet, M., Mariotti, A., Lange-Badre, B., Vandermeersch, B., Borel, J.P. et al. (1991) Isotopic biogeochemistry (^{13}C,^{15}N) of fossil vertebrate collagen: application to the study of a past food web including Neandertal man. *Journal of Human Evolution*, 20, 481–492.

Bocherens, H., Fizet, M., Mariotti, A., Gangloff, R.A. & Burns, J.A. (1994) Contribution of isotopic biogeochemistry ^{13}C, ^{15}N, ^{18}O to the paleoecology of mammoths (*Mammuthus primigenius*). *Historical Biology*, 7, 187–202.

Bocherens, H., Pacaud, G., Lazarev, P.A. & Mariotti, A. (1996) Stable isotope abundances (^{13}C, ^{15}N) in collagen and soft tissues from Pleistocene mammals from Yakutia: implications for the palaeobiology of the Mammoth Steppe. *Palaeogeography, Palaeoclimatology, Palaeoecology*, 126(1/2), 31–44.

Bocherens, H., Billiou, D., Mariotti, A., Toussaint, M., Patou-Mathis, M., Bonjean, D. et al. (2001) New isotopic evidence for dietary habits of Neandertals from Belgium. *Journal of Human Evolution*, 40, 497–505.

Bonafini, M., Pellegrini, M., Ditchfield, P. & Pollard, A.M. (2013) Investigation of the 'canopy effect' in the isotope ecology of temperate woodlands. *Journal of Archaeological Science*, 40(11), 3926–3935.

Bogaard, A., Heaton, T.H.E., Poulton, P. & Merbach, I. (2007) The impact of manuring on nitrogen isotope ratios in cereals: archaeological implications for reconstruction of diet and crop management practices. *Journal of Archaeological Science*, 34(3), 335–343.

Bösl, C., Grupe, G. & Peters, J. (2006) A Late Neolithic vertebrate food web based on stable isotope analyses. *International Journal of Osteoarchaeology*, 16, 296–315.

Brandtner, F. (1990) Die Paläolithstation "Grubgraben" bei Kammern. Vorläufige Ergebnisse neuerer Grabungen. *Fundberichte aus Österreich*, 28(1989), 17–26.

Brandtner, F. (1996) Zur geostratigraphischen und kulturellen Zuordnung der Paläolithstation Grubgraben bei Kammern, NÖ. In: Svoboda, J. (Ed) *Paleolithic in the Middle Danube Region* vol. 4. Brno: festschrift for B. Klíma, *Dolní Věstonice Studies*. pp. 121–146.

Britton, K. (2010) Multi-isotope analysis and the reconstruction of prey species palaeomigrations and palaeoecology. Doctoral dissertation, Durham University.

Britton, K., Gaudzinski-Windheuser, S., Roebroeks, W., Kindler, L. & Richards, M.P. (2012) Stable isotope analysis of well-preserved 120,000-year-old herbivore bone collagen from the Middle Palaeolithic site of Neumark-Nord 2, Germany reveals niche separation between bovids and equids. *Palaeogeography, Palaeoclimatology, Palaeoecology*, 333-334, 168–177.

Britton, K., Grimes, V., Niven, L., Steele, T.E., McPherron, S., Soressi, M. et al. (2011) Strontium isotope evidence for migration in late Pleistocene Rangifer: implications for Neanderthal hunting strategies at the Middle Palaeolithic site of Jonzac, France. *Journal of Human Evolution*, 61(2), 176–185.

Brock, F., Higham, T. & Ramsey, C.B. (2010) Pre-screening techniques for identification of samples suitable for radiocarbon dating of poorly preserved bones. *Journal of Archaeological Science*, 37, 855–865.

Bronk Ramsey, C. (2009) Bayesian analysis of radiocarbon dates. *Radiocarbon*, 51(1), 337–360.

Caboń-Raczyńska, K., Krasińska, M. & Krasiński, Z. (1983) Behaviour and daily activity rhythm of European bison in winter. *Acta Theriologica*, 28(18), 273–299.

Caboń-Raczyńska, K., Krasińska, M., Krasiński, Z.A. & Wójcik, J.M. (1987) Bisoniana XCVII. Rhythm of daily activity and behavior of European bison in the Białowieża Forest in the period without snow cover. *Acta Theriologica*, 32(21), 335–372.

Cersoy, S., Zazzo, A., Lebon, M., Rofes, J. & Zirah, S. (2016) Collagen extraction and stable isotope analysis of small vertebrate bones: a comparative approach. *Radiocarbon*, 59, 679–694. Available at: https://doi.org/10.1017/RDC.2016.82

Cichocki, O., Knibbe, B. & Tillich, I. (2014) Archaeological significance of the Palaeolithic charcoal assemblage from Krems-Wachtberg. *Quaternary International*, 351, 163–171.

Coltrain, J.B., Harris, J.M., Cerling, T.E., Ehleringer, J.R., Dearing, M.D., Ward, J. et al. (2004) Rancho La Brea stable isotope biogeochemistry and its implications for the palaeoecology of late Pleistocene, coastal southern California. *Palaeogeography, Palaeoclimatology, Palaeoecology*, 205, 199–219.

Coplen, T.B. (2011) Guidelines and recommended terms for expression of stable-isotope-ratio and gas-ratio measurement results. *Rapid Communications in Mass Spectrometry*, 25, 2538–2560.

Craine, J.M., Elmore, A.J., Wang, L., Augusto, L., Baisden, W.T., Brookshire, E.N.J. et al. (2015) Convergence of soil nitrogen isotopes across global climate gradients. *Scientific Reports*, 5, 8280. Available at: https://doi.org/10.1038/srep08280

Dale Guthrie, R. (2001) Origin and causes of the mammoth steppe: a story of cloud cover, woolly mammal tooth pits, buckles, and inside-out Beringia. *Quaternary Science Reviews*, 20(1-3), 549–574.

Delisle, G., Grassmann, S., Cramer, B., Messner J. & Winsemann, J. (2007) Estimating episodic permafrost development in northern Germany during the Pleistocene. In: *Sedimentary Processes and Products, Part 3 Quaternary Glacial Systems*, Hambrey M.J., Christoffersen P., Glasser N.F. (Eds.) International Association of Sedimentologists, Blackwell Publishing Ltd: Malden, Oxford, Victoria; 109–119.

DeNiro, M.J. (1985) Postmortem preservation and alteration of in vivo bone collagen isotope ratios in relation to palaeodietary reconstruction. *Nature*, 317, 806–809.

DeNiro, M.J. & Epstein, S. (1978) Influence of diet on the distribution of carbon isotopes in animals. *Geochimica et Cosmochimica Acta*, 42, 495–506. Available at: https://doi.org/10.1016/0016-70377890199-0

DeNiro, M.J. & Epstein, S. (1981) Influence of diet on the distribution of nitrogen isotopes in animals. *Geochimica et Cosmochimica Acta*, 45, 341–351. Available at: https://doi.org/10.1016/0016-70378190244-1

DeNiro, M.J. & Weiner, S. (1988) Chemical, enzymatic and spectroscopic characterization of "collagen" and other organic fractions from prehistoric bones. *Geochimica et Cosmochimica Acta*, 52, 2197–2206.

Dobberstein, R.C., Collins, M.J., Craig, O.E., Taylor, G., Penkman, K.E.H. & Ritz-Timme, S. (2009) Archaeological collagen: Why worry about collagen diagenesis. *Archaeological and Anthropological Sciences*, 1, 31–42. Available at: https://doi.org/10.1007/s12520-009-0002-7

Drucker, D., Bocherens, H., Cleyet-Merle, J.J., Madelaine, S., Mariotti, A. (2000) Implications paléoenvironnementales de l'étude isotopique (^{13}C, ^{15}N) de la faune des grands mammifères des Jamblancs (Dordogne, France)/Isotopic study (^{13}C, ^{15}N) of large mammal fauna from Les Jamblancs (Dordogne, France): paleoenvironnemental implications. *Paléo*, 12, 127–140.

Drucker, D.G. (2022) The isotopic ecology of the mammoth steppe. *Annual Review of Earth and Planetary Sciences*, 50, 395–418.

Drucker, D.G., Bocherens, H. & Billiou, D. (2003) Evidence for shifting environmental conditions in Southwestern France from 33,000 to 15,000 years ago derived from carbon-13 and nitrogen-15 natural abundances in collagen of large herbivores. *Earth and Planetary Science Letters*, 216, 163–173.

Drucker, D., Bocherens, H., Pike-Tay, A. & Mariotti, A. (2001) Isotopic tracking of seasonal dietary change in dentine collagen: preliminary data from modern caribou. *Comptes Rendus de l'Académie des Sciences - Series IIA - Earth and Planetary Science*, 333, 303–309.

Drucker, D.G., Bridault, A. & Cupillard, C. (2012) Environmental context of the Magdalenian settlement in the Jura Mountains using stable isotope tracking (^{13}C, ^{15}N, ^{34}S) of bone collagen from reindeer (*Rangifer tarandus*). *Quaternary International*, 272-273, 322–332.

Drucker, D.G., Bridault, A., Hobson, K.A., Szuma, E. & Bocherens, H. (2008) Can carbon-13 in large herbivores reflect the canopy effect in temperate and boreal ecosystems? Evidence from modern and ancient ungulates. *Palaeogeography, Palaeoclimatology, Palaeoecology*, 266, 69–82.

Drucker, D.G. & Henry-Gambier, D. (2005) Determination of the dietary habits of a Magdalenian woman from Saint-Germain-la-Rivière in southwestern France using stable isotopes. *Journal of Human Evolution*, 49, 19–35.

Drucker, D.G., Kind, C.J. & Stephan, E. (2011) Chronological and ecological information on Late-glacial and early Holocene reindeer from northwest Europe using radiocarbon (^{14}C) and stable isotope (^{13}C, ^{15}N) analysis of bone collagen: Case study in southwestern Germany. *Quaternary International*, 245, 218–224.

Drucker, D.G., Stevens, R.E., Germonpré, M., Sablin, M.V., Péan, S. & Bocherens, H. (2018) Collagen stable isotopes provide insights into the end of the mammoth steppe in the central East European plains during the Epigravettian. *Quaternary Research*, 90, 457–469.

Drucker, D.G., Vercoutère, C., Chiotti, L., Nespoulet, R., Crépin, L., Conard, N.J. et al. (2015) Tracking possible decline of woolly mammoth during the Gravettian in Dordogne (France) and the Ach Valley (Germany) using multi-isotope tracking (^{13}C, ^{14}C, ^{15}N, ^{34}S, ^{18}O). *Quaternary International*, 359-360, 304–317.

Duprat-Oualid, F., Rius, D., Bégeot, C., Magny, M., Millet, L., Wulf, S. et al. (2017) Vegetation response to abrupt climate changes in Western Europe from 45 to 14.7k cal a BP: the Bergsee lacustrine record (Black Forest, Germany): vegetation response to climate change, Black Forest. *Journal of Quaternary Science*, 32(7), 1008–1021.

Dytham, C. (2011) *Choosing and using Statistics. A biologist's guide*, Third Edition. West Sussex: Wiley Blackwell.

Einwögerer, T. (2000) Die jungpaläolithische Station auf dem Wachtberg in Krems, NÖ. Eine Rekonstruktion und wissenschaftliche Darlegung der Grabung von J. Bayer aus dem Jahre 1930. Mitteilungen der Prähistorischen Kommission 34, Wien.

Einwögerer, T. (2019) Langenlois Fundstelle A. Verlag der Österreichischen Akademie der Wissenschaften 88, pp. 206.

Einwögerer, T., Händel, M., Neugebauer-Maresch, C., Simon, U., Steier, P., Teschler-Nicola, M. et al. (2009) ^{14}C Dating of the Upper Paleolithic Site at Krems-Wachtberg, Austria. *Radiocarbon*, 51, 847–855.

Evans, R.D. (2001) Physiological mechanisms influencing plant nitrogen isotope composition. *Trends in Plant Science*, 6(3), 121–126.

Farquhar, G.D., Ehleringer, J.R. & Hubick, K.T. (1989) Carbon isotope discrimination and photosynthesis. *Annual Review of Plant Physiology and Plant Molecular Biology*, 40(1), 503–537.

Fedosenko, A.K. & Blank, D.A. (2001) Capra sibirica. *Mammalian Species*, 675, 1–13.

Finstad, G.L. & Kielland, K. (2011) Landscape Variation in the Diet and Productivity of Reindeer in Alaska Based on Stable Isotope Analyses. *Arctic, Antarctic, and Alpine Research*, 43(4), 543–554.

Fizet, M., Mariotti, A., Bocherens, H., Lange-Badré, B., Vandermeersch, B., Borel, J.P. et al. (1995) Effect of diet, physiology and climate on carbon and nitrogen stable isotopes of collagen in a late pleistocene anthropic palaeoecosystem: Marillac, Charente, France. *Journal of Archaeological Science*, 22, 67–79.

Fladerer, F.A. (2001) Die Faunareste vom jungpaläolithischen Lagerplatz Krems-Wachtberg, Ausgrabung 1930: jagdwild und Tierkörpernutzung an der Donau vor 27000 Jahren. Verlag der Österreichischen Akademie der Wissenschaften.

Fladerer, F.A. & Salcher-Jedrasiak, T. (2008) Krems-Hundssteig 2000-2002: archäozoologische und taphonomische Untersuchungen. In: *Krems-Hundssteig – Mammutjäger der Eiszeit. Ein Nutzungsareal paläolithischer Jäger- und Sammlerinnen vor 41.000-27.000 Jahren*, Neugebauer-Maresch, C. (ed). Mitteilungen der Prähistorischen Kommission: Wien; 67: 216–312.

Fontana, L. (2017) The four seasons of reindeer: non-migrating reindeer in the Dordogne region (France) between 30 and 18k? Data from the Middle and Upper Magdalenian at La Madeleine and methods of seasonality determination. *Journal of Archaeological Science: Reports*, 12, 346–362.

Fox-Dobbs, K., Bump, J.K., Peterson, R.O., Fox, D.L. & Koch, P.L. (2007) Carnivore-specific stable isotope variables and variation in the foraging ecology of modern and ancient wolf populations: case studies from Isle Royale, Minnesota, and La Brea. *Canadian Journal of Zoology*, 85, 458–471.

Fox-Dobbs, K., Leonard, J.A. & Koch, P.L. (2008) Pleistocene megafauna from eastern Beringia: paleoecological and paleoenvironmental interpretations of stable carbon and nitrogen isotope and radiocarbon records. *Palaeogeography, Palaeoclimatology, Palaeoecology*, 261, 30–46.

Fraser, R.A., Bogaard, A., Heaton, T., Charles, M., Jones, G., Christensen, B.T. et al. (2011) Manuring and stable nitrogen isotope ratios in cereals and pulses: towards a new archaeobotanical approach to the inference of land use and dietary practices. *Journal of Archaeological Science*, 38(10), 2790–2804.

Georgi, M., Voerkelius, S., Rossmann, A., Graßmann, J. & Schnitzler, W.H. (2005) Multielement isotope ratios of vegetables from integrated and organic production. *Plant and Soil*, 275, 93–100.

Germonpré, M., Sablin, M.V., Stevens, R.E., Hedges, R.E.M., Hofreiter, M., Stiller, M. et al. (2009) Fossil dogs and wolves from Palaeolithic sites in Belgium, the Ukraine and Russia: osteometry, ancient DNA and stable isotopes. *Journal of Archaeological Science*, 36, 473–490.

Gilot, E. 1997. Index général des dates LV. Laboratoire du Carbone 14 de Louvain/Louvain-la-Neuve. Studia Praehistorica Belgica 7, Liège.

Grupe, G., Mikic, Z., Peters, J. & Manhart, H. (2003) Vertebrate food webs and subsistence strategies of Meso- and Neolithic populations of central Europe. *Documenta Archaeobiologia*, 1, 193–213.

Guiry, E.J. & Szpak, P. (2021) Improved quality control criteria for stable carbon and nitrogen isotope measurements of ancient bone collagen. *Journal of Archaeological Science*, 132, 105416.

Guthrie, R.D. (1982) Mammals of the mammoth steppe as paleoenvironmental indicators. In: Moody Hopkins, D. (Ed.) *Paleoecology of Beringia*. New York: Academic. pp. 307–326.

Haesaerts, P., Damblon, F., Neugebauer-Maresch, C. & Einwögerer, T. (2016) Radiocarbon Chronology of the Late Palaeolithic Loess Site of Kammern-Grubgraben (Lower Austria). *Archaeologia Austriaca*, 1, 271–280.

Haesaerts, P. (1990) Stratigraphy of the Grubgraben Loess Sequence. In: Montet-White, A. (Ed.) *The Epigravettian site of Grubgraben, Lower Austria: The 1986 and 1987 excavations*, 40. Liège: ERAUL: Université de Liège. pp. 15–35.

Händel, M. (2017) The stratigraphy of the Gravettian sites at Krems. *Quartär*, 64, 129–155.

Händel, M., Simon, U., Maier, A., Brandl, M., Groza-Săcaciu, S.M., Timar-Gabor, A. et al. (2021a) Kammern-Grubgraben revisited – First results from renewed investigations at a well-known LGM site in east Austria. *Quaternary International*, 587–588, 137–157. Available at: https://doi.org/10.1016/j.quaint.2020.06.012

Händel, M., Thomas, R., Sprafke, T., Schulte, P., Brandl, M., Simon, U. et al. (2021b) Using archaeological data and sediment parameters to review the formation of the Gravettian layers at Krems-Wachtberg. *Journal of Quaternary Science*, 36(8), 1397–1413.

Handley, L.L., Austin, A.T., Robinson, D., Scrimgeour, C.M., Raven, J.A., Heaton, T.H.E. et al. (1999) The ^{15}N natural abundance ($\delta^{15}N$) of ecosystem samples reflects measures of water availability. *Australian Journal of Plant Physiology*, 26(2), 185–199.

Hedges, R.E.M., Clement, J.G., Thomas, C.D.L. & O'Connell, T.C. (2007) Collagen turnover in the adult femoral mid-shaft: modeled from anthropogenic radiocarbon tracer measurements. *American Journal of Physical Anthropology*, 133(2), 808–816.

Heinrich, W. 1973. Das Jungpalolithikum in Niederosterreich. Unpublished dissertation, University of Salzburg.

Heiri, O., Koinig, K.A., Spötl, C., Barrett, S., Brauer, A., Drescher-Schneider, R. et al. (2014) Palaeoclimate records 60–8 ka in the Austrian and Swiss Alps and their forelands. *Quaternary Science Reviews*, 106, 186–205.

Hobson, K.A. (1999) Tracing origins and migration of wildlife using stable isotopes: a review. *Oecologia*, 120, 314–326.

Högberg, P. (1997) Tansley Review No. 95. ^{15}N natural abundance in soil-plant systems. *New Phytologist*, 137(2), 179–203.

Hoke, N., Rott, A., Johler, S., Reul, A., Beck, A., Günther, A. et al. (2019) How bone degradation, age, and collagen extraction methods affect stable isotope analysis. *Archaeological and Anthropological Sciences*, 11, 3357–3374.

Iacumin, P., Bocherens, H., Delgado Huertas, A., Mariotti, A. & Longinelli, A. (1997) A stable isotope study of fossil mammal remains from the Paglicci cave, Southern Italy. N and C as palaeoenvironmental indicators. *Earth and Planetary Science Letters*, 148(1-2), 349–357.

Iacumin, P., Davanzo, S. & Nikolaev, V. (2006) Spatial and temporal variations in the $^{13}C/^{12}C$ and $^{15}N/^{14}N$ ratios of mammoth hairs: palaeodiet and palaeoclimatic implications. *Chemical Geology*, 231, 16–25.

Iacumin, P., Di Matteo, A., Nikolaev, V. & Kuznetsova, T.V. (2010) Climate information from C, N and O stable isotope analyses of mammoth bones from northern Siberia. *Quaternary International*, 212(2), 206–212.

Iacumin, P., Nikolaev, V. & Ramigni, M. (2000) C and N stable isotope measurements on Eurasian fossil mammals, 40 000 to 10 000 years bp: Herbivore physiologies and palaeoenvironmental reconstruction. *Palaeogeography, Palaeoclimatology, Palaeoecology*, 163, 33–47.

Jackson, A.L., Inger, R., Parnell, A.C. & Bearhop, S. (2011) Comparing isotopic niche widths among and within communities: SIBER – Stable Isotope Bayesian Ellipses in R. *Journal of Animal Ecology*, 80, 595–602.

Kaczensky, P., Ganbaatar, O., von Wehrden, H. & Walzer, C. (2008) Resource selection by sympatric wild equids in the Mongolian Gobi. *Journal of Applied Ecology*, 45, 1762–1769.

Kämpf, L., Rius, D., Duprat-Oualid, F., Crouzet, C. & Millet, L. (2022) Evidence for wind patterns and associated landscape response in Western Europe between 46 and 16 ka cal. BP. *Quaternary Science Reviews*, 298, 107846.

Kindler, P., Guillevic, M., Baumgartner, M., Schwander, J., Landais, A. & Leuenberger, M. (2014) Temperature reconstruction from 10 to 120 kyr b2k from the NGRIP ice core. *Climate of the Past*, 10(2), 887–902.

Kirillova, I.V., Argant, J., Lapteva, E.G., Korona, O.M., van der Plicht, J., Zinovyev, E.V. et al. (2016) The diet and environment of mammoths in North-East Russia reconstructed from the contents of their feces. *Quaternary International*, 406, 147–161.

Kohn, M.J. (2010) Carbon isotope compositions of terrestrial C_3 plants as indicators of (paleo)ecology and (paleo)climate. *Proceedings of the National Academy of Sciences*, 107(46), 19691–19695.

Krajcarz, M., Pacher, M., Krajcarz, M.T., Laughlan, L., Rabeder, G., Sabol, M. et al. (2016) Isotopic variability of cave bears ($\delta^{15}N$, $\delta^{13}C$) across Europe during MIS 3. *Quaternary Science Reviews*, 131, 51–72.

Krajcarz, M.T., Krajcarz, M. & Bocherens, H. (2018) Collagen-to-collagen prey-predator isotopic enrichment ($\Delta^{13}C$, $\Delta^{15}N$) in terrestrial mammals - a case study of a subfossil red fox den. *Palaeogeography, Palaeoclimatology, Palaeoecology*, 490, 563–570.

Kristensen, D.K., Kristensen, E., Forchhammer, M.C., Michelsen, A. & Schmidt, N.M. (2011) Arctic herbivore diet can be inferred from stable carbon and nitrogen isotopes in C_3 plants, faeces, and wool. *Canadian Journal of Zoology*, 89(10), 892–899.

Kronfeld-Schor, N., Shargal, E., Haim, A., Dayan, T., Zisapel, N. & Heldmaier, G. (2001) Temporal partitioning among diurnally and nocturnally active desert spiny mice: energy and water turnover costs. *Journal of Thermal Biology*, 26, 139–142.

Lambert, J.B., Gronert, S., Shurvell, H.F., Lightner, D. & Gronert, S. (1998). Organic structural spectroscopy. Pearson College Division.

Lebon, M., Reiche, I., Gallet, X., Bellot-Gurlet, L. & Zazzo, A. (2016) Rapid quantification of bone collagen content by ATR-FTIR spectroscopy. *Radiocarbon*, 58, 131–145.

Luetscher, M., Boch, R., Sodemann, H., Spötl, C., Cheng, H., Edwards, R.L. et al. (2015) North Atlantic storm track changes during the last glacial maximum recorded by alpine speleothems. *Nature Communications*, 6, 6344.

Ma, J., Fengli, Z., Yuan, W. & Yaowu, H. (2017). Tracking the foraging behavior of *Mammuthus primigenius* from the late Pleistocene of northeast China, using stable isotope analysis. *Quaternary Science* 37(4): 885–894.

Ma, J., Wang, Y., Baryshnikov, G.F., Drucker, D.G., McGrath, K., Zhang, H. et al. (2021) The *Mammuthus-Coelodonta* Faunal Complex at its southeastern limit: a biogeochemical paleoecology investigation in Northeast Asia. *Quaternary International*, 591, 93–106.

Maier, A., Stojakowits, P., Mayr, C., Pfeifer, S., Preusser, F., Zolitschka, B. et al. (2021) Cultural evolution and environmental change in Central Europe between 40 and 15 ka. *Quaternary International*, 581-582, 225–240.

Mayewski, P.A., Meeker, L.D., Twickler, M.S., Whitlow, S., Yang, Q., Lyons, W.B. et al. (1997) Major features and forcing of high-latitude northern hemisphere atmospheric circulation using a 110,000-year long glaciochemical series. *Journal of Geophysical Research: Oceans*, 102, 26345–26366.

Mix, A. (2001) Environmental processes of the ice age: land, oceans, glaciers (EPILOG). *Quaternary Science Reviews*, 20(4), 627–657.

Moine, O., Antoine, P., Hatté, C., Landais, A., Mathieu, J., Prud'homme, C. et al. (2017) The impact of Last Glacial climate variability in west-European loess revealed by radiocarbon dating of fossil earthworm granules. *Proceedings of the National Academy of Sciences*, 114(24), 6209–6214.

Montet-White, A. (1988) Recent excavations at Grubgraben. A Gravettian site in Lower Austria. *Archäologisches Korrespondenzblatt*, 18, 213–218.

Montet-White, A. (1990). The Epigravettian Site of Grubgraben, Lower Austria: the 1986 and 1987 Excavations. *ERAUL Études et Recherche Archéologiques de l´Université de Liège* 40, Liège.

Munizzi, J.S. (2017). Rethinking Holocene ecological relationships among caribou, muskoxen, and human hunters on Banks Island, NWT, Canada: a stable isotope approach. PhD Dissertation, University of Western Ontario: London, Ontario, Canada.

Nadachowski, A., Lipecki, G., Baca, M., Żmihorski, M. & Wilczyński, J. (2018) Impact of climate and humans on the range dynamics of the woolly mammoth (Mammuthus primigenius) in Europe during MIS 2. *Quaternary Research*, 90, 439–456.

Nadelhoffer, K., Shaver, G., Fry, B., Giblin, A., Johnson, L., McKane, R. (1996) ^{15}N natural abundances and N use by tundra plants. *Oecologia*, 107(3), 386–394.

Naito, Y.I., Chikaraishi, Y., Drucker, D.G., Ohkouchi, N., Semal, P., Wißing, C. et al. (2016) Ecological niche of Neanderthals from Spy Cave revealed by nitrogen isotopes of individual amino acids in collagen. *Journal of Human Evolution*, 93, 82–90.

Neugebauer-Maresch, C. & Cichocki, O. (2008) Holzbefunde. In: Neugebauer-Maresch, C. (Ed.) *Krems-Hundssteig – Mammutjägerlager der Eiszeit. Ein Nutzungsareal paläolithischer Jager- und Sammler(-innen) vor 41.000-27.000 Jahren*, 67. Wien: Mitteilungen der Prähistorischen Kommission. pp. 147–167.

Neugebauer-Maresch, C., Einwögerer, T., Richter, J., Maier, A. & Hussain, S.T. (2016) Kammern-Grubgraben. Neue Erkenntnisse zu den Grabungen 1985–1994. *Archaeologia Austriaca*, 1, 225–254. Available at: https://doi.org/10.1553/archaeologia100s225

Neugebauer-Maresch, C., Peticzka, R., Frank, C. (2008) Stratigraphie und Befunde. In: Neugebauer-Maresch, C. (Ed.) *Krems-Hundssteig – Mammutjägerlager der Eiszeit. Ein Nutzungsareal paläolithischer Jager- und Sammler(-innen) vor 41.000-27.000 Jahren*, Mitteilungen der Prähistorischen Kommission: Wien; 67: 68–146.

Neugebauer-Maresch, C. & Stadler, P. (2008) Absolute Datierung. In: Neugebauer-Maresch, C. (Ed.) *Krems-Hundssteig –Mammutjägerlager der Eiszeit. Ein Nutzungsareal paläolithischer Jager- und Sammler(-innen) vor 41.000-27.000 Jahren*, 67. Wien: Mitteilungen der Prähistorischen Kommission. pp. 168–176.

Obermaier, H. (1908) Die am Wagramdurchbruch des Kamp gelegenen niederösterreichischen Quartärfundplätze. *Jahrbuch für Altertumskunde*, II, 49–85.

Parrini, F., Cain, III, J.W. & Krausman, P.R. (2009) *Capra ibex* (Artiodactyla: Bovidae). *Mammalian Species*, 830, 1–12.

Pataki, D.E., Ehleringer, J.R., Flanagan, L.B., Yakir, D., Bowling, D.R., Still, C.J. et al. (2003) The application and interpretation of Keeling plots in terrestrial carbon cycle research. *Global Biogeochemical Cycles*, 17(1), 1022. Available at: https://doi.org/10.1029/2001GB001850

Pfeifer, S., Pasda, K., Händel, M. et al. accepted. The osseous industry of the LGM site Kammern-Grubgraben (Lower Austria), excavations 1985-1994, and its position within the European Late Upper Palaeolithic. *Quartär*.

Rasmussen, S.O., Bigler, M., Blockley, S.P., Blunier, T., Buchardt, S.L., Clausen, H.B. et al. (2014) A stratigraphic framework for abrupt climatic changes during the Last Glacial period based on three synchronized Greenland ice-core records: refining and extending the INTIMATE event stratigraphy. *Quaternary Science Reviews*, 106, 14–28.

Reimer, P.J., Austin, W.E.N., Bard, E., Bayliss, A., Blackwell, P.G., Ramsey, C.B. et al. (2020) The IntCal20 Northern Hemisphere. *Radiocarbon Age Calibration Curve (0–55 cal kBP). Radiocarbon*, 62, 725–757.

Reiss, L., Stüwe, C., Einwögerer, T., Händel, M., Maier, A., Meng, S. et al. (2022) Evaluation of geochemical proxies and radiocarbon data from a loess record of the Upper Palaeolithic site Kammern-Grubgraben, Lower Austria. *E&G Quaternary Science Journal*, 71, 23–43.

Richards, M.P. & Hedges, R.E.M. (2003) Variations in bone collagen $\delta^{13}C$ and $\delta^{15}N$ values of fauna from Northwest Europe over the last 40000 years. *Palaeogeography, Palaeoclimatology, Palaeoecology*, 193, 261–267.

Řičánková, V.P., Robovský, J., Riegert, J. & Zrzavý, J. (2015) Regional patterns of postglacial changes in the Palearctic mammalian diversity indicate retreat to Siberian steppes rather than extinction. *Scientific Reports*, 5, 12682. Available at: https://doi.org/10.1038/srep12682

Scheibe, K.M., Eichhorn, K., Kalz, B., Streich, W.J. & Scheibe, A. (1998) Water consumption and watering behavior of przewalski horses (*Equus ferus przewalskii*) in a semireserve. *Zoo Biology*, 17, 181–192.

Schoeninger, M.J. & DeNiro, M.J. (1984) Nitrogen and carbon isotopic composition of bone collagen from marine and terrestrial animals. *Geochimica et Cosmochimica Acta*, 48, 625–639.

Schwartz-Narbonne, R., Longstaffe, F.J., Kardynal, K.J., Druckenmiller, P., Hobson, K.A., Jass, C.N. et al. (2019) Reframing the mammoth steppe: insights from analysis of isotopic niches. *Quaternary Science Reviews*, 215, 1–21.

Schwartz-Narbonne, R., Longstaffe, F.J., Metcalfe, J.Z. & Zazula, G. (2015) Solving the woolly mammoth conundrum: amino acid ^{15}N-enrichment suggests a distinct forage or habitat. *Scientific Reports*, 5(1), 9791.

Spöttl, I. (1890) Resultate der Ausgrabungen für die Anthropologische Gesellschaft in NÖ und in Mähren im Jahre 1889. *Mitteilungen der Anthropologischen Gesellschaft Wien* XX.

Sprafke, T., Schulte, P., Meyer-Heintze, S., Händel, M., Einwögerer, T., Simon, U. et al. (2020) Paleoenvironments from robust loess stratigraphy using high-resolution color and grain-size data of the last glacial Krems-Wachtberg record (NE Austria. *Quaternary Science Reviews*, 248, 106602. Available at: https://doi.org/10.1016/j.quascirev.2020.106602

Stevens, R.E. & Hedges, R.E.M. (2004) Carbon and nitrogen stable isotope analysis of northwest European horse bone and tooth collagen, 40,000 bp-present: palaeoclimatic interpretations. *Quaternary Science Reviews*, 23(7–8), 977–991.

Stevens, R.E., Jacobi, R., Street, M., Germonpré, M., Conard, N.J., Münzel, S.C. et al. (2008) Nitrogen isotope analyses of reindeer (*Rangifer tarandus*), 45,000 BP to 9,000 BP: palaeoenvironmental reconstructions. *Palaeogeography, Palaeoclimatology, Palaeoecology*, 262(1–2), 32–45.

Stevens, R.E., O'Connell, T.C., Hedges, R.E.M., Street, M. (2009) Radiocarbon and stable isotope investigations at the Central Rhineland sites of Gönnersdorf and Andernach-Martinsberg, Germany. *Journal of Human Evolution*, 57, 131–148.

Stewart, K.M., Bowyer, R.T., Kie, J., Dick, B.L., Ben-David, M. (2003) Niche partitioning among mule deer, elk, and cattle: do stable isotopes reflect dietary niche? *ÉCOSCIENce*, 10(3), 297–302.

Stojakowits, P., Mayr, C., Ivy-Ochs, S., Preusser, F., Reitner, J.M. & Spötl, C. (2021) Environments at the MIS 3/2 transition in the northern Alps and their foreland. *Quaternary International*, 581-582, 99–113.

Stojakowits, P., Mayr, C., Lücke, A., Wissel, H., Hedenäs, L., Lempe, B. et al. (2020) Impact of climatic extremes on Alpine ecosystems during MIS 3. *Quaternary Science Reviews*, 239, 106333. Available at: https://doi.org/10.1016/j.quascirev.2020

Szpak, P., Gröcke, D.R., Debruyne, R., MacPhee, R.D.E., Dale Guthrie, R., Froese, D., et al. (2010) Regional differences in bone collagen $\delta^{13}C$ and $\delta^{15}N$ of Pleistocene mammoths: implications for paleoecology of the mammoth steppe. *Palaeogeography, Palaeoclimatology, Palaeoecology* 286(1-2): 88–96.

Terhorst, B., Kühn, P., Damm, B., Hambach, U., Meyer-Heintze, S. & Sedov, S. (2014) Paleoenvironmental fluctuations as recorded in the loess-paleosol sequence of the Upper Paleolithic site Krems-Wachtberg. *Quaternary International*, 351, 67–82.

Tieszen, L.L. (1991) Natural variations in the carbon isotope values of plants: implications for archaeology, ecology, and paleoecology. *Journal of Archaeological Science*, 18, 227–248.

van Klinken, G.J. (1999) Bone Collagen Quality Indicators for Palaeodietary and Radiocarbon Measurements. *Journal of Archaeological Science*, 26, 687–695.

Vandenberghe, J., French, H.M., Gorbunov, A., Marchenko, S., Velichko, A.A., Jin, H. et al. (2014) The Last Permafrost Maximum (LPM) map of the Northern Hemisphere: permafrost extent and mean annual air temperatures, 25-17 ka BP: The Last Permafrost Maximum (LPM) map of the Northern Hemisphere. *Boreas*, 43, 652–666.

Voelker, A.H.L. & workshop participants. (2002) Global distribution of centennial-scale records for Marine Isotope Stage (MIS) 3: a database. *Quaternary Science Reviews*, 21, 1185–1212.

Wang, G., Han, J., Zhou, L., Xiong, X. & Wu, Z. (2005) Carbon isotope ratios of plants and occurrences of C_4 species under different soil moisture regimes in arid region of Northwest China. *Physiologia Plantarum*, 125, 74–81.

Wang, Y. & Wooller, M.J. (2006) The stable isotopic (C and N) composition of modern plants and lichens from northern Iceland: with ecological and paleoenvironmental implications. *Jökull*, 56, 27–37.

Werner, R.A. & Schmidt, H.L. (2002) The in vivo nitrogen isotope discrimination among organic plant compounds. *Phytochemistry*, 61, 465–484.

Wooller, M.J., Bataille, C., Druckenmiller, P., Erickson, G.M., Groves, P., Haubenstock, N. et al. (2021) Lifetime mobility of an Arctic woolly mammoth. *Science*, 373(6556), 806–808.

Yeakel, J.D., Guimarães Jr., P.R., Bocherens, H. & Koch, P.L. (2013) The impact of climate change on the structure of Pleistocene food webs across the mammoth steppe. *Proceedings of the Royal Society B: Biological Sciences*, 280, 20130239.

Zimov, S.A., Chuprynin, V.I., Oreshko, A.P., Chapin, F.S., Reynolds, J.F., Chapin, M.C. (1995) Steppe-tundra transition: a herbivore-driven biome shift at the end of the Pleistocene. *The American Naturalist*, 146(5), 765–794.

Zimov, S.A., Zimov, N.S., Tikhonov, A.N. & Chapin, F.S. (2012) Mammoth steppe: a high-productivity phenomenon. *Quaternary Science Reviews*, 57, 26–45.